

# **Relation of Fracture Orientation to Linear Terrain Features, Anisotropic Transmissivity, and Seepage to Streams in the Karst Prairie du Chien Group, Southeastern Minnesota**

**By James F. Ruhl**

---

**U.S. Geological Survey  
Water-Resources Investigations Report 94-4146**

**Prepared in Cooperation with the**

**Minnesota Department of Natural Resources and  
Legislative Commission on Minnesota Resources**



**Mounds View, Minnesota  
1995**

**U.S. DEPARTMENT OF THE INTERIOR**

**BRUCE BABBITT, Secretary**

**U.S. GEOLOGICAL SURVEY**

**Gordon P. Eaton, Director**

---

For additional information  
write to:

District Chief  
U.S. Geological Survey  
2280 Woodale Drive  
Mounds View, MN 55112

Copies of this report can  
be purchased from:

U.S. Geological Survey  
Earth Science Information Center  
Open-File Reports Section  
Box 25286, MS 517  
Denver Federal Center  
Denver, Colorado 80225

## Contents

Abstract .....	1
Introduction .....	1
Purpose and scope .....	2
Previous investigations.....	2
Physical setting.....	4
Methods of data collection and analysis .....	5
Fracture orientation .....	5
Linear terrain features .....	5
Anisotropy of transmissivity .....	9
Seepage rates .....	9
Relation of linear terrain features to fracture orientation.....	11
Relation of anisotropy of transmissivity to fracture orientation .....	11
Relation of linear terrain features to seepage.....	26
Summary .....	40
References.....	41

## Illustrations

Figure 1. Generalized hydrogeologic column showing regional aquifers and confining units in southeastern Minnesota .....	3
2-3. Maps showing:	
2. Study area including subcrop of the Prairie du Chien-Jordan Formations in southeastern Minnesota.....	4
3. Locations of outcrop sites in the Prairie du Chien Group in southeastern Minnesota, boundaries of areas surrounding these sites where linear terrain features were mapped, and location of aquifer-test site .....	6
4. Photograph showing examples of features on a 1:80,000 black and white aerial photograph that were mapped as linear terrain features .....	7
5. Map showing seepage-measurement sites and boundaries of surrounding areas where linear terrain features were mapped in the Prairie du Chien Group in southeastern Minnesota .....	8
6. Diagram showing locations of observation wells in relation to the pumping well used in the aquifer test of the karst portion of the St. Peter-Prairie du Chien-Jordan aquifer conducted November 12, 1989 near Rochester, Minnesota, and generalized section of the pumping well .....	10
7a-7b. Maps showing:	
7a. Stream channel reaches used to measure seepage rates at four seepage-measurement sites in southeastern Minnesota .....	12
7b. Stream channel reaches used to measure seepage rates at two seepage-measurement sites in southeastern Minnesota .....	14

## Illustrations--Continued

8-17. Maps showing linear terrain features and rose diagrams of these features and of fracture orientation measurements for:	
8. Exposure site 1 of the Prairie du Chien Group in southeastern Minnesota.....	15
9. Exposure site 2 of the Prairie du Chien Group in southeastern Minnesota.....	16
10. Exposure site 3 of the Prairie du Chien Group in southeastern Minnesota.....	17
11. Exposure site 4 of the Prairie du Chien Group in southeastern Minnesota.....	18
12. Exposure site 5 of the Prairie du Chien Group in southeastern Minnesota.....	19
13. Exposure site 6 of the Prairie du Chien Group in southeastern Minnesota.....	20
14. Exposure site 7 of the Prairie du Chien Group in southeastern Minnesota.....	21
15. Exposure site 8 of the Prairie du Chien Group in southeastern Minnesota.....	22
16. Exposure site 9 of the Prairie du Chien Group in southeastern Minnesota.....	23
17. Exposure site 10 of the Prairie du Chien Group in southeastern Minnesota.....	24
18-19. Graphs showing:	
18. Drawdown at each of three observation wells during pumping of a production well at 240 gal/min (gallons per minute) for an aquifer test of the Prairie du Chien-Jordan aquifer conducted on November 12, 1989, near Rochester, Minnesota.....	27
19. The relation of the type curve $[W(\mu)+\bar{f}]$ versus $1/\mu$ determined for a partially penetrating production well discharging at a constant rate of 240 gal/min (gallons per minute) from a nonleaky aquifer with a vertical to radial anisotropy of 100 to the time versus drawdown curve for three observation wells used in an aquifer test of the Prairie du Chien-Jordan aquifer conducted on November 12, 1989, near Rochester, Minnesota.....	28
20. Map showing rose diagram and linear terrain features in the area surrounding the seepage-measurement sites along the Middle Fork of the Zumbro River.....	29
21a. Map showing linear terrain features in the area surrounding the seepage-measurement sites along the Middle Fork of the Zumbro River.....	30

## Illustrations--Continued

21b. Rose diagram of the linear terrain features in the area surrounding the seepage-measurement sites along the South Branch of the Middle Fork of the Zumbro River .....	31
22a. Map showing linear terrain features in the area surrounding the seepage-measurement sites along Crow Creek and the Middle Fork of the Whitewater River.....	32
22b. Rose diagram of the linear terrain features in the area surrounding the seepage measurement sites along Crow Creek and the Middle Fork of the Whitewater River.....	33
23a. Map showing linear terrain features in the area surrounding the seepage-measurement sites along the South Branch of the Root River .....	34
23b. Rose diagram of the linear terrain features in the area surrounding the seepage-measurement sites along the South Branch of the Root River .....	35
24a. Map showing linear terrain features in the area surrounding the seepage-measurement sites along Duschee Creek .....	36
24b. Rose diagram of the linear terrain features in the area surrounding the seepage-measurement sites along Duschee Creek .....	37
25a. Map showing linear terrain features in the area surrounding the seepage-measurement sites along Riceford Creek .....	38
25b. Rose diagram of the linear terrain features in the area surrounding the seepage-measurement sites along Riceford Creek .....	39

## Tables

Table	1. Seepage rates along stream reaches at six sites .....	25
	2. Chi square statistic computed for fracture orientation measurements collected at ten exposure sites in the Prairie du Chien Group and for linear terrain feature data interpreted from aerial photographs of areas that surround the exposure sites.....	26
	3. Chi square statistic computed for linear terrain feature data interpreted from aerial photographs of areas shown in figure 5 for each of the seepage-measurement sites .....	40

## Conversion Factors and Abbreviations

<u>Multiply inch-pound unit</u>	<u>By</u>	<u>To obtain SI Unit</u>
foot (ft)	0.3048	meter
square foot per day (ft <sup>2</sup> /d)	.09290	square meter per day
cubic foot per second (ft <sup>3</sup> /s)	.02832	cubic meter per second
gallon (gal)	3.785	liter
gallon per minute (gal/min)	.06308	liter per second
mile (mi)	1.609	kilometer
square mile (mi <sup>2</sup> )	2.590	square kilometer

**Township, range, and section:** In this report, the system used to denote locations is based on the U.S. Bureau of Land Management's system of land subdivision (township, range, and section). Thus, the site location T109NR14W10 is in township 109 north, range 14 west, section 10.

**Sea level** In this report "sea level" refers to the National Geodetic Vertical Datum of 1929 (NGVD of 1929)—a geodetic datum derived from a general adjustment of the first-order level nets of both the United States and Canada, formerly called "Sea Level Datum of 1929".

# **Relation of Fracture Orientation to Linear Terrain Features, Anisotropic Transmissivity, and Seepage to Streams in the Karst Prairie du Chien Group, Southeastern Minnesota**

**by James F. Ruhl**

## **Abstract**

Ground-water flow in the karst-terrane aquifers of southeastern Minnesota is not well defined. Variable fracture patterns in the bedrock affect permeability. Techniques to predict the effects of fracture patterns on ground-water flow in the karst-terrane aquifers of southeastern Minnesota are unavailable. The use of such techniques may be useful to officials responsible for the management and protection of ground water in these aquifers, which have a high susceptibility to contamination. The U.S. Geological Survey, in cooperation with the Minnesota Department of Natural Resources and the Legislative Commission on Minnesota Resources, investigated fracture patterns, anisotropic transmissivity, and seepage to streams from the Prairie du Chien Group, which is the karst portion of the St. Peter-Prairie du Chien-Jordan aquifer, to improve the understanding of ground-water flow through karst-terrane aquifers in southeastern Minnesota.

This report presents the results of testing hypotheses that (1) the major axes of linear terrain features correlate with the major axes of subsurface fractures in the Prairie du Chien Group, and that (2) the major axes of subsurface fractures in the Prairie du Chien Group correlate with seepage from the Prairie du Chien Group.

The first hypothesis was tested by comparison of linear terrain features to fracture orientation measurements. Fracture orientations in 10 exposures of the Prairie du Chien Group at quarries, road cuts, and natural outcrops showed statistically significant directional trends at 8 of 10 sites. Directional trends of linear terrain features identified from 1:80,000 aerial photographs were significant in four of the ten 60-square mile areas that surround these sites. The fracture orientation measurements correlate with the local linear terrain features in 2 of the 10 sites.

The second hypothesis was tested by analyzing the correlation between seepage rates into streams hydraulically connected to the Prairie du Chien Group and surrounding linear terrain features that were mapped in approximately 300 square mile areas. Data from Riceford Creek support this hypothesis; data from Crow Creek and Middle Fork of the Whitewater River and from Duschee Creek are inconclusive. This hypothesis could not be tested by the data from the Middle Fork of the Zumbro River, the South Branch of the Root River, and the South Branch of the Middle Fork of the Zumbro River because the surrounding linear terrain features lack directional trends.

The transmissivity of the karst portion of the St. Peter-Prairie du Chien-Jordan aquifer is anisotropic at an aquifer-test site in the study area. Results of the aquifer test indicate that the major axis of transmissivity is along a line N95°E. The aquifer-test results indicate that the principal axis of joint fractures at the test site is slightly clockwise from an east-west line because this axis is assumed to correlate with the major axis of horizontal transmissivity.

## **Introduction**

Ground-water flow in the karst-terrane aquifers of southeastern Minnesota is not well defined. Variable fracture patterns in the bedrock affect permeability. Techniques to predict the effects of fracture patterns on ground-water flow in the karst-terrane aquifers of southeastern Minnesota are unavailable. The use of such techniques may be useful to officials responsible

for the management and protection of ground water in these aquifers, which have a high susceptibility to contamination (Porcher, 1989). The U.S. Geological Survey, in cooperation with the Minnesota Department of Natural Resources and the Legislative Commission on Minnesota Resources, investigated fracture patterns, anisotropic transmissivity, and seepage to streams in the karst Prairie du Chien Group, to improve the

understanding of ground-water flow through karst-terrane aquifers in southeastern Minnesota.

Karst-terrane, carbonate rock aquifers in southeastern Minnesota have permeability from fractures, solution channels, and gaps between bedding planes. Water moves through these aquifers and gradually dissolves the rock. Ground-water movement then shifts from slow and diffuse flow to rapid and concentrated flow through the openings in the rock. Sinkholes and caves form where carbonate rock aquifers are at or near land surface. Where the water table drops below the surface of streams, conditions exist for streams to lose water to the aquifer and decrease in flow, or disappear altogether.

The principal carbonate rock aquifer in southeastern Minnesota is the St. Peter-Prairie du Chien-Jordan aquifer, comprised of the St. Peter Sandstone, the Prairie du Chien Group, and Jordan Sandstone. The Prairie du Chien Group is the karst portion of this aquifer. This aquifer is part of a sequence of sedimentary rocks that are present throughout southeastern Minnesota (fig. 1).

This report presents results of tests of the following hypotheses: (1) the major axes of linear terrain features correlate with the major axes of subsurface fractures in the Prairie du Chien Group, and (2) these major axes of subsurface fractures correlate with seepage from the Prairie du Chien Group. The hypotheses were tested by analysis of fracture orientations in the Prairie du Chien Group, local linear terrain features, and seepage rates into streams incised into the Prairie du Chien Group.

### **Purpose and Scope**

The report describes (1) the relation of linear terrain features to orientation of fractures in the Prairie du Chien Group in southeastern Minnesota, and (2) the relation of anisotropy of transmissivity of the karst portion of the St. Peter-Prairie du Chien-Jordan aquifer to fractures in the Prairie du Chien Group, and (3) the relation of linear terrain features to seepage from the Prairie du Chien Group to streams. The study area includes Wabasha, Olmsted, Winona, Fillmore, and Houston Counties, located in southeastern Minnesota (fig. 2). Fracture orientation data were collected in the subcrop of the Prairie du Chien Group. The subcrop of the Prairie du Chien-Jordan Formations shown in figure 2 extends slightly beyond but closely approximates the subcrop of the Prairie du Chien Group (Dale Setterholm, Minnesota Geological Survey, written commun., 1995). The fracture orientations were determined by field measurements at 10 sites where the Prairie du Chien Group was exposed. Linear terrain features were identified on 1:80,000 aerial photographs within 60 mi<sup>2</sup> areas surrounding the 10 exposure sites. An aquifer test


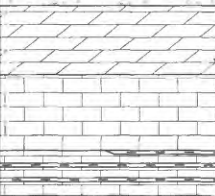
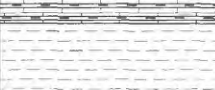

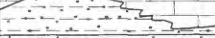

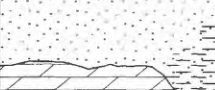
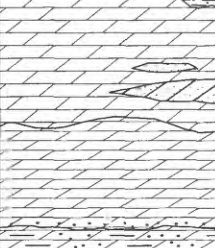


was done to determine the anisotropy of the transmissivity in the karst portion of the St. Peter-Prairie du Chien-Jordan aquifer. Seepage from the Prairie du Chien Group was analyzed from base-flow data collected at six seepage-measurement sites. Seepage rates were determined for two to five stream channel reaches at each of the six seepage-measurement sites and compared to linear terrain features within surrounding 300 mi<sup>2</sup> areas.

### **Previous Investigations**

Detailed descriptions of fracture patterns in southeastern Minnesota are unavailable. Some site-specific investigations, however, provide information about local conditions. Mossler and Book (1984) reported that the only known fault in Winona County has an east-west orientation. Fracture orientation data from a landfill study in Winona County indicate that the most common joint directions in the Oneota Dolomite, Prairie du Chien Group, and Jordan Sandstone, are about N110°E and are about N50°E (Dalgleish and Alexander, 1984). Olsen (1988) determined that the direction of joints in glacial till and in bedrock in Olmsted County are about N180°E to N160°E and are about N70°E to N50°E.

Mossler and Book (1984) reported that stream valleys in Winona County probably are aligned with the direction of joints. The orientation of these valleys generally is north-south and northeast-southwest; however, the orientation of some valleys, particularly those that drain secondary and tertiary streams in the watersheds, is random. Olsen (1988) reported that erosional patterns in stream valleys of Olmsted County indicate dominant northwest-southeast or northeast-southwest jointing patterns and less prominent north-south orientation.

Regional ground-water-flow directions in southeastern Minnesota are toward the major rivers (Delin and Woodward, 1984). Movement of ground water in the St. Peter-Prairie du Chien-Jordan aquifer is toward the Mississippi River on a regional scale. Locally, ground water in this aquifer is likely to move in many directions toward stream discharge areas, which include the Root, Whitewater, and Zumbro Rivers (Broussard and others, 1975). No studies have been done on local ground-water flow in the St. Peter-Prairie du Chien-Jordan aquifer in southeastern Minnesota. However, tracer studies conducted on near-surface flow in the Upper Carbonate aquifer have shown that water travels as much as 12 miles along flow paths that diverge, change directions, and cross surface-drainage divides (Mohring and Alexander, 1986).

ERATHEM	SYSTEM OR SERIES	FORMATION OR GROUP	THICKNESS (IN FEET)	GENERAL LITHOLOGY	WATER-BEARING CHARACTERISTICS
CENOZOIC	QUATERNARY	UNDIFFERENTIATED GLACIAL DRIFT	0-450		UNDIFFERENTIATED GLACIAL DRIFT AQUIFER AND CONFINING UNIT--Glacial drift serves as a confining unit to underlying formations in some areas, and as an aquifer in others. Aquifers are used primarily for domestic and farm supply throughout area and for municipal supply along the western boundary. Drift consists of till, alluvium, buried and surficial outwash, valley train, lake, terrace, and ice-contact deposits.
		GALENA FORMATION	0-210		UPPER CARBONATE AQUIFER--Limited to south central part of Hollandale Embayment in Minnesota, where it is the most extensively used aquifer. Permeability is attributed to extensive karst development. Yields to municipal wells range from 200 to 500 gal/min. Horizontal hydraulic conductivity generally ranges from 3 to 40 feet per day.
PALEOZOIC	ORDOVICIAN	DECORAH SHALE	0-90		DECORAH-PLATTEVILLE-GLENWOOD CONFINING UNIT--Small quantities of water from fractures and solution cavities may be obtained locally from the Platteville. Vertical hydraulic conductivity is about 10 feet per day.
		PLATTEVILLE FORMATION	0-30		
		GLENWOOD SHALE	0-16		
		ST. PETER SANDSTONE	0-130		ST. PETER AQUIFER--Yields typically range from 100 to 250 gal/min, but yields of 1,200 gal/min have been obtained. Sandstone is poorly cemented, and wells tend to fill with sand. Horizontal hydraulic conductivity is 15 to 20 feet per day.
			0-65		BASAL ST. PETER CONFINING UNIT--Siltstone and shale in basal St. Peter restricts vertical flow. Absent in Olmsted County.
		PRAIRIE DU CHIEN GROUP	0-310		PRAIRIE DU CHIEN-JORDAN AQUIFER--Most extensively used aquifer in southeastern Minnesota. Yields range from 500 to 1,000 gal/min. Hydraulic conductivity is due to joints, fractures, and solution cavities in the Prairie du Chien and coarse-grained sandstone in the Jordan. Horizontal hydraulic conductivity generally ranges from 1 to 40 feet per day, and can be greater than 1,000 feet per day locally.
		SHAKOPEE FORMATION			
		ONEOTA DOLOMITE			
		COON VALLEY MEMBER	0-25		
	CAMBRIAN	JORDAN SANDSTONE	90-130		

Hydrogeology from Delin and Woodward, 1984.

#### EXPLANATION OF GENERAL LITHOLOGY


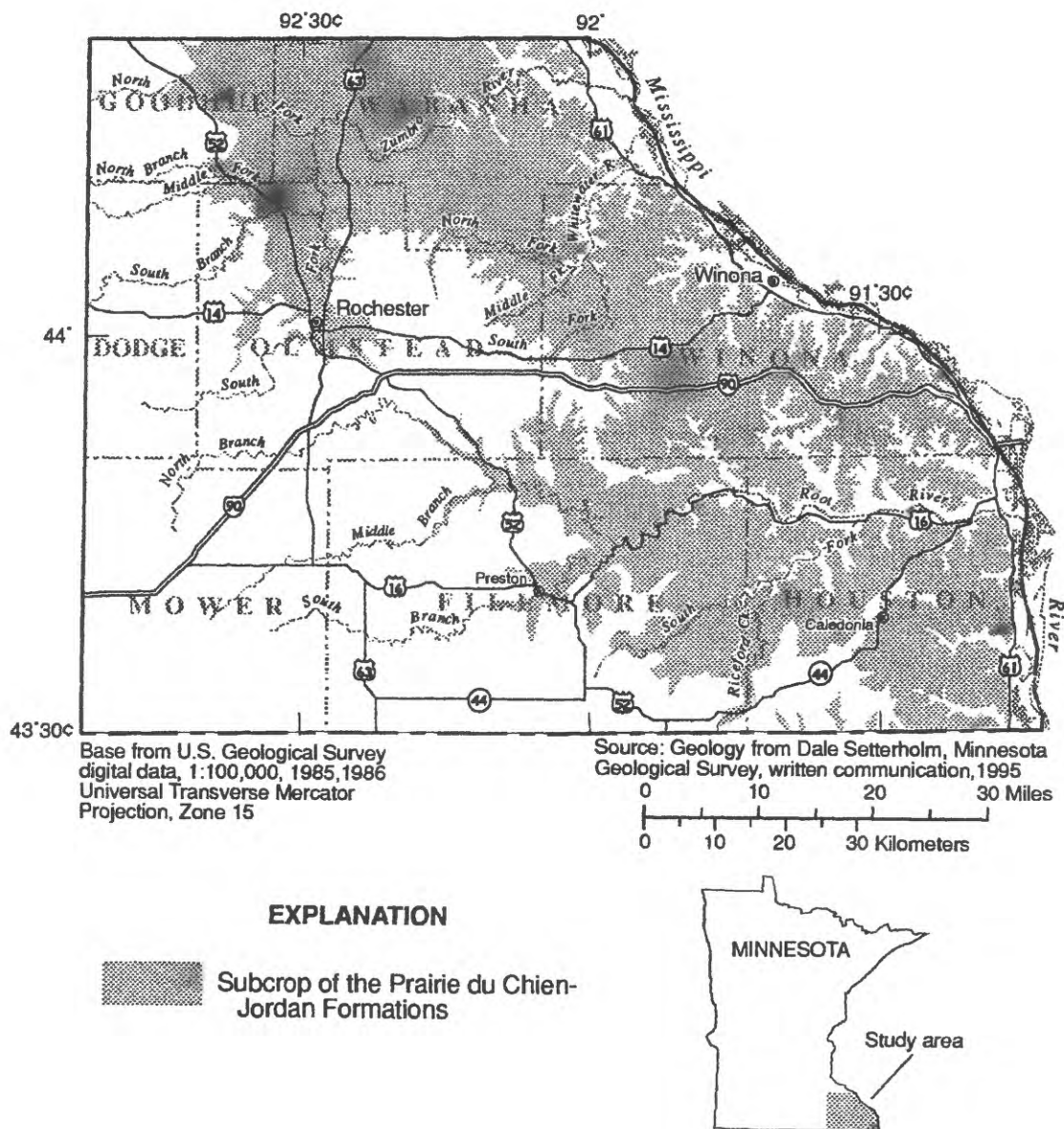
	Till, sand, and gravel		Limestone		Sandstone		Dolomite		Shale
---	------------------------	---	-----------	---	-----------	---	----------	---	-------

Figure 1.--Generalized hydrogeologic column showing regional aquifers and confining units in southeastern Minnesota.



**Figure 2.—Study area including subcrop of the Prairie du Chien-Jordan Formations in southeastern Minnesota.**

### Physical Setting

Karst topography has developed in southeastern Minnesota where carbonate rock formations underlie thin layers of unconsolidated surficial material. Caves, sinkholes, and disappearing streams, which are

landscape features typical of karst topography, are present in southeastern Minnesota.

Quaternary sediments in southeastern Minnesota include loess of Wisconsin age (about 25,000 to 10,000 years ago) and pre-Wisconsin glacial till that overlie bedrock plateaus. The Quaternary sediments also

include 3 types of till of pre-Illinoian age (older than 300,000 years) in Olmsted County (Hobbs, 1988). Weathering of bedrock formed a clayey sand that thickens eastward toward the Mississippi River. The clayey sand is interbedded with the loess and till and probably underwent transport and redeposition (Hobbs, 1984). Alluvium of Wisconsin age and valley-fill materials that consist of clay, silt, sand, and gravel are in flood plains and in adjacent lowlands (Broussard and others, 1975). These deposits are as much as 150 ft thick in the Mississippi River Valley.

Bedrock outcrops are widespread in southeastern Minnesota. The resistance of the bedrock to erosion controlled the development of stream drainage patterns and much of the bedrock topography of the region (Olsen, 1988). Streams have eroded channels of variable size and slope through the sedimentary rocks and have formed bedrock outcrops along the valley walls. Carbonate rocks are more resistant to erosion than the shales and sandstones; consequently, limestone and dolomite crop out beneath unconsolidated material over a large area of southeastern Minnesota. Differential erosion has formed plateaus on top of escarpments and bluffs where carbonate rocks overlie less resistant bedrock.

The Decorah-Platteville-Glenwood confining unit restricts movement of water between the Upper Carbonate and St. Peter-Prairie du Chien-Jordan aquifers. Seeps and springs are present where the contact between the confining unit and the Upper Carbonate aquifer is at or near land surface. The locations of springs and seeps are at the base of valley walls, although some are in karst upland areas. Springs and seeps that stop flowing during dry periods probably are recharged by local flow systems, and those that flow continuously probably are recharged by regional flow systems (Kanivetsky, 1984). The recharge primarily is from precipitation and snowmelt on subcrops of the aquifers followed by infiltration through the Quaternary sediments.

## Methods of Data Collection and Analysis

Direct measurements of fracture orientation in the Prairie du Chien Group were made with a compass at ten outcrops. Linear terrain features were identified on 1:80,000 aerial photographs of areas that surround the outcrops. The correlation between fracture orientations and directional trends of linear terrain features was then analyzed. Base flow was measured to determine seepage rates along two to five reaches of streams incised into the Prairie du Chien Group at six seepage-measurement sites. The correlation between seepage rates and

directional trends of linear terrain features was then analyzed.

### Fracture Orientation

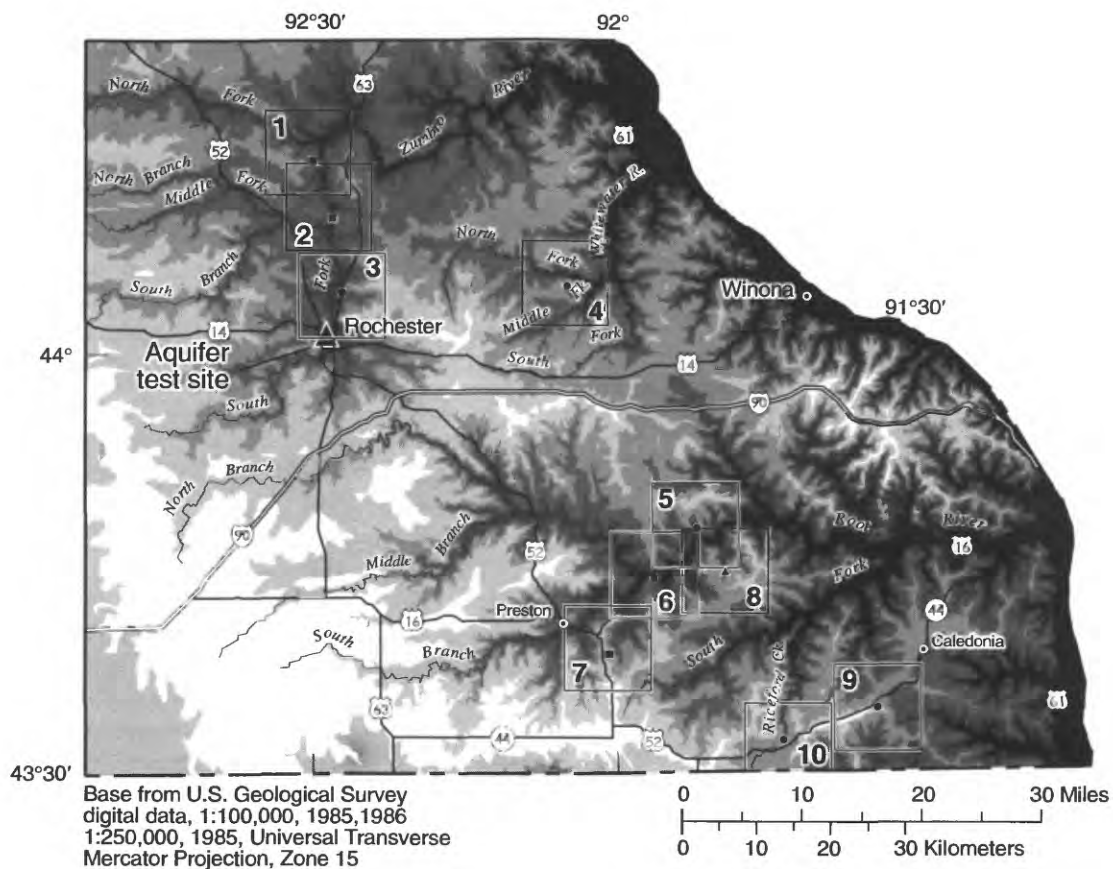
Approximately 30 to 80 fracture orientation measurements were made at each of 10 sites where the Prairie du Chien Group crops out at quarries, stream valleys, and road cuts (fig. 3). Measurements were made of the orientation of vertical openings that ranged from one-fourth to several inches in width. Quarries provided the best source of data because of the full exposure of bedrock surfaces.

### Linear Terrain Features

Linear terrain features are distinguished by length. Lattman (1958) defined lineaments as features at least one mile in length and fracture traces as features less than one mile in length. These features, which include stream valleys, ridges, vegetational boundaries, and lines of demarcation between soils of different color tone, may indicate subsurface fracture zones (Lattman, 1958). Linear terrain features have been identified and mapped in many kinds of terrane, including karst (Lattman and Parizek, 1964). Although these features are often inconspicuous on the ground, these features can be identified on aerial photographs. Examples of linear terrain features mapped for this study area are shown on the aerial photograph in figure 4.

Linear terrain features mapped in this study predominantly are straight segments of stream valleys and well defined drainage paths down the hillsides of these stream valleys. Linear terrain features mapped along major stream valleys such as the Root, Whitewater, and Zumbro Rivers, were weighted more strongly than features mapped along small streams and along hillside erosional features. The frequency of observations along the major stream valleys was increased by a factor of three. Approximately 90 percent of the mapped linear terrain features are major and minor stream valleys and hillside drainage paths. The remainder of the linear terrain features are expressions of vegetational patterns and soil color.

Ten areas of about 60 mi<sup>2</sup> each were used to map linear terrain features around outcrops of the Prairie du Chien Group (fig. 3). Six areas of about 300 mi<sup>2</sup> each were used to map linear terrain features around six seepage-measurement sites (fig. 5). The number of features within each area around an outcrop ranged from 31 to 110, and the number of features around each seepage-measurement site ranged from 154 to 423, a sufficient number to perform the chi square test for statistical significance of directional trends. The areas



### EXPLANATION

- 8  
▲

 Stream valley
- 9  
•

 Quarry
- 1  
▪

 Road cut

Number next to symbols are site identifiers. The square outlines around each symbol delineate boundaries of the site lineament maps.

Elevation above sea level

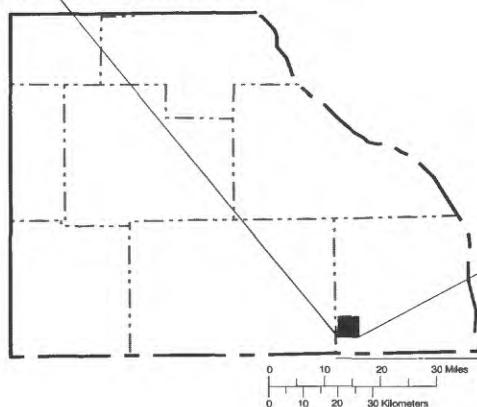
FEET	METERS
1509	460
1411	430
1312	400
1214	370
1116	340
1017	310
919	280
820	250
722	220
610	186

**Figure 3.--Locations of outcrop sites in the Prairie du Chien Group in southeastern Minnesota, boundaries of areas surrounding these sites where linear terrain features were mapped, and location of aquifer test site.**



Aerial photography from The National  
High Altitude Photography Program,  
Department of Interior, 1982

0 0.5 1 1.5 2 Miles  
0 0.5 1 1.5 2 Kilometers

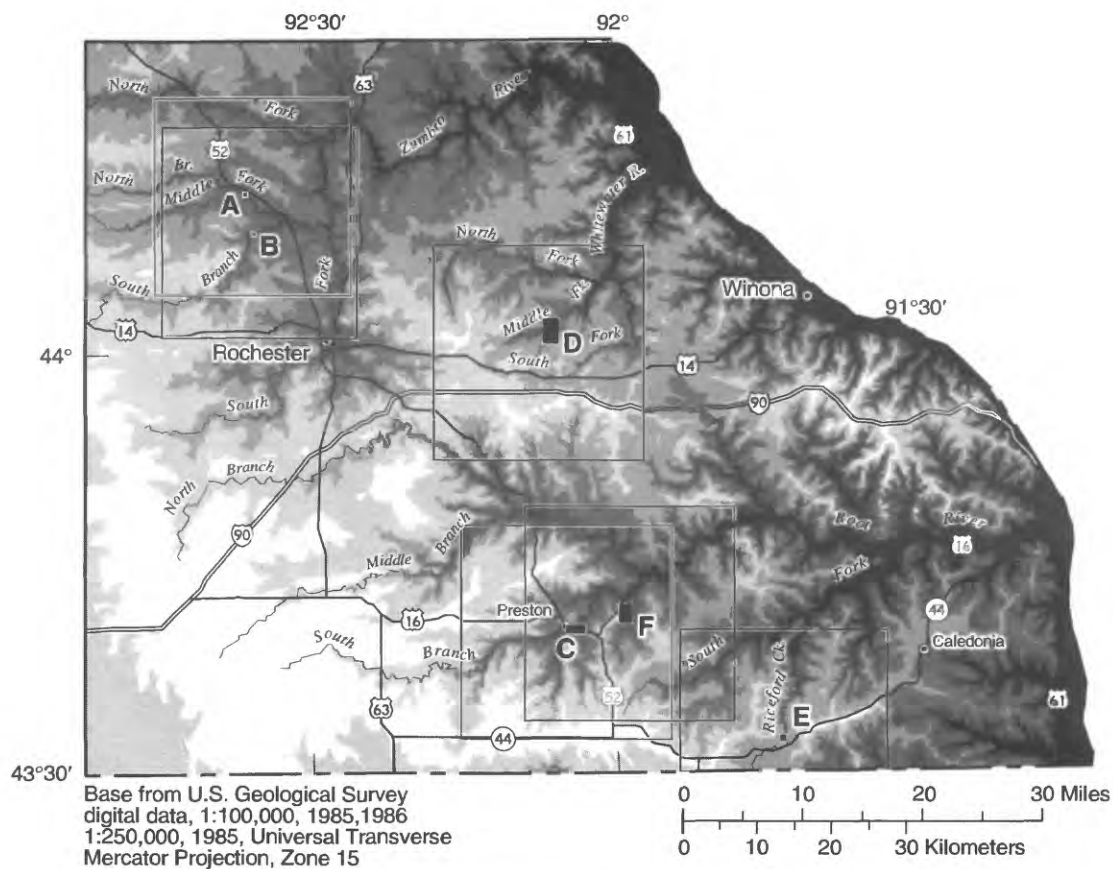


#### EXPLANATION



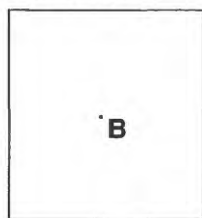
Delineates a feature mapped as  
a linear terrain feature.

**Figure 4.--Examples of features on a 1:80,000 black and white aerial  
photograph that were mapped as linear terrain features.**



### EXPLANATION

Solid rectangle and letter designates seepage-measurement site. Square line around each seepage measurement site defines boundary of surrounding area where linear terrain features were mapped.



- A** Middle Fork of Zumbro River
- B** South Branch of Middle Fork of Zumbro River
- C** South Branch of Root River
- D** Crow Creek and Middle Fork of Whitewater River
- E** Riceford Creek
- F** Duschee Creek

Elevation above sea level

FEET	METERS
1509	460
1411	430
1312	400
1214	370
1116	340
1017	310
919	280
820	250
722	220
610	186

**Figure 5.—Seepage-measurement sites and boundaries of surrounding areas where linear terrain features were mapped in the Prairie du Chien Group in southeastern Minnesota.**

used to map linear terrain features are larger around the seepage measurement sites than around the outcrops because the seepage-measurement sites extend over larger areas than the outcrops.

## Anisotropy of Transmissivity

An aquifer test designed to determine the anisotropic transmissivity—the directional variation of the ability of an aquifer to transmit water—of the karst portion of the St. Peter-Prairie du Chien-Jordan aquifer was conducted on a well completed in the Prairie du Chien Group in Rochester, Minnesota (fig. 3). The direction of maximum transmissivity was assumed to correlate with the principal axis of joint fractures in the rocks.

Commercial drillers' logs indicate that the Prairie du Chien Group underlies 40 to 45 ft of silty clay with some sand and gravel at the test site. In the region of the aquifer test site the thickness of the Prairie du Chien Group is about 300 ft, and the thickness of the underlying Jordan Sandstone is about 100 ft (Olsen, 1988).

Three observation wells used for the aquifer test were located in each of three quadrants about 225 to 500 ft from the pumping well (fig. 6). The U.S. Geological Survey installed observation wells A and C at a depth of 150 ft. Well casings were installed in wells A and C to the top of the bedrock. Below the top of the bedrock, the boreholes of wells A and C were left open to the Prairie du Chien Group. The pumping well and observation well B, which are privately owned, were completed to a depth of 250 ft and cased approximately 10 ft into the Prairie du Chien Group. The boreholes of the pumping well and well B were left open to the Prairie du Chien Group below the bottom of the casing. The pumping well and three observation wells penetrated only part of the St. Peter-Prairie du Chien-Jordan aquifer, which is about 400 ft thick at the test site.

The analysis of the aquifer test data assumed three-dimensional flow through the Prairie du Chien Group toward the pumping well without leakage from the overlying unconsolidated material. The type curves of  $[W(\mu) + \bar{f}]$  versus  $1/\mu$  were generated from equations developed by Hantush (1964, p. 353), and were solved by a computer program published by Reed (1980, p. 9). The relation of the drawdown in the observation wells to the pumping rate, transmissivity, and well function  $[W(\mu) + \bar{f}]$ , is defined by the following equation:

$$s = \frac{Q}{4\pi T} \left[ W(\mu) + \bar{f} \left( \mu, \frac{a}{b}, \frac{l}{b}, \frac{d}{b}, \frac{l'}{b}, \frac{d'}{b} \right) \right] \quad (1)$$

where,

$s$  = drawdown (L),

$Q$  = flow rate [ $L^3T^{-1}$ ],

$T$  = transmissivity [ $L^2T^{-1}$ ],

$W(\mu)$  = well function [dimensionless],

$\mu$  = argument in the well function [dimensionless],

$r$  = distance from pumped well to observational well (L),

$a$  = square root of the ratio of the vertical to horizontal hydraulic conductivity, commonly

expressed as  $\sqrt{\frac{K_z}{K_r}}$  [dimensionless],

$b$  = aquifer thickness (L),

$l$  = depth from top of aquifer to bottom of pumped well screen (L),

$d$  = depth from top of aquifer to top of pumped well screen (L),

$b'$  = thickness of confining unit overlying the aquifer (L),

$l'$  = depth from top of aquifer to bottom of observation well screen (L),

$d'$  = depth from top of aquifer to top of observation well screen (L),

$\bar{f}$  = correction factor function for partial penetration of both the pumping well and observation wells.

The well function  $[W(\mu) + \bar{f}]$  corrects for partial penetration of both the pumping well and observation wells. Type curves computed for vertical to radial anisotropy of 100 were fitted to the measured time-series drawdown data for each of the three observation wells. Match points for drawdown ( $s$ ), time ( $t$ ),  $\mu$ , and  $[W(\mu) + \bar{f}]$  were determined. The equations used to determine the major and minor axes of horizontal anisotropy were formulated by Papadopoulos (1965). A computer program developed by Maslia and Randolph (1987) was used to solve the equations formulated by Papadopoulos (1965). This computer program calculates the transmissivities along the major and minor axes of transmissivity, determines the directions of the major and minor axes of transmissivity, and the storage coefficient.

## Seepage Rates

Seepage rates were measured during base-flow conditions in late summer 1988 along two to five reaches of streams incised into the Prairie du Chien Group at six seepage-measurement sites (table 1). Seepage-measurement sites were selected that best fit the following criteria: (1) presence of stream channel reaches hydraulically connected to the Prairie du Chien Group indicated by exposures of these rocks either in

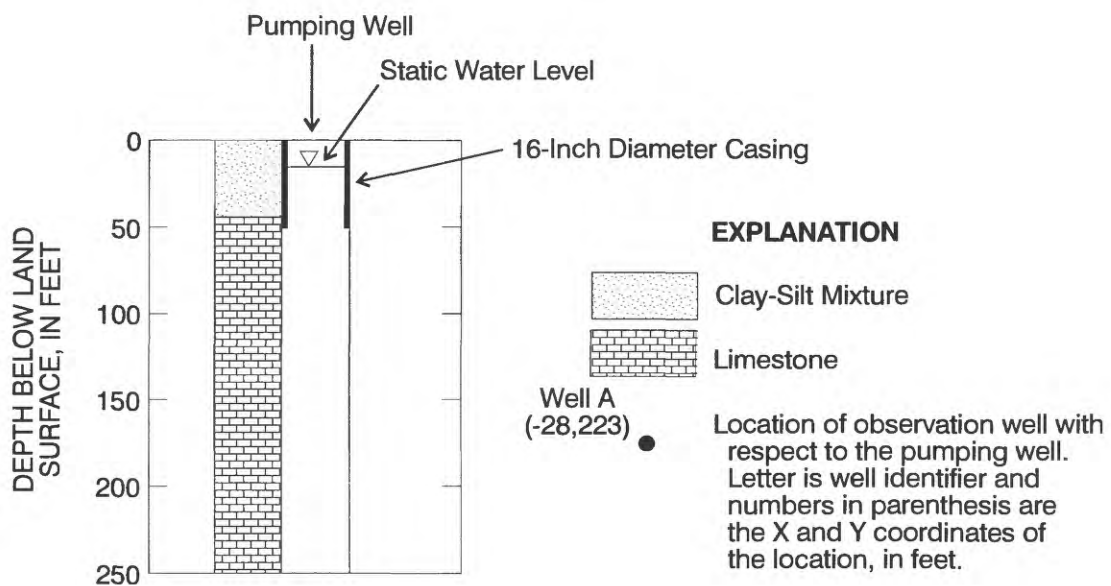
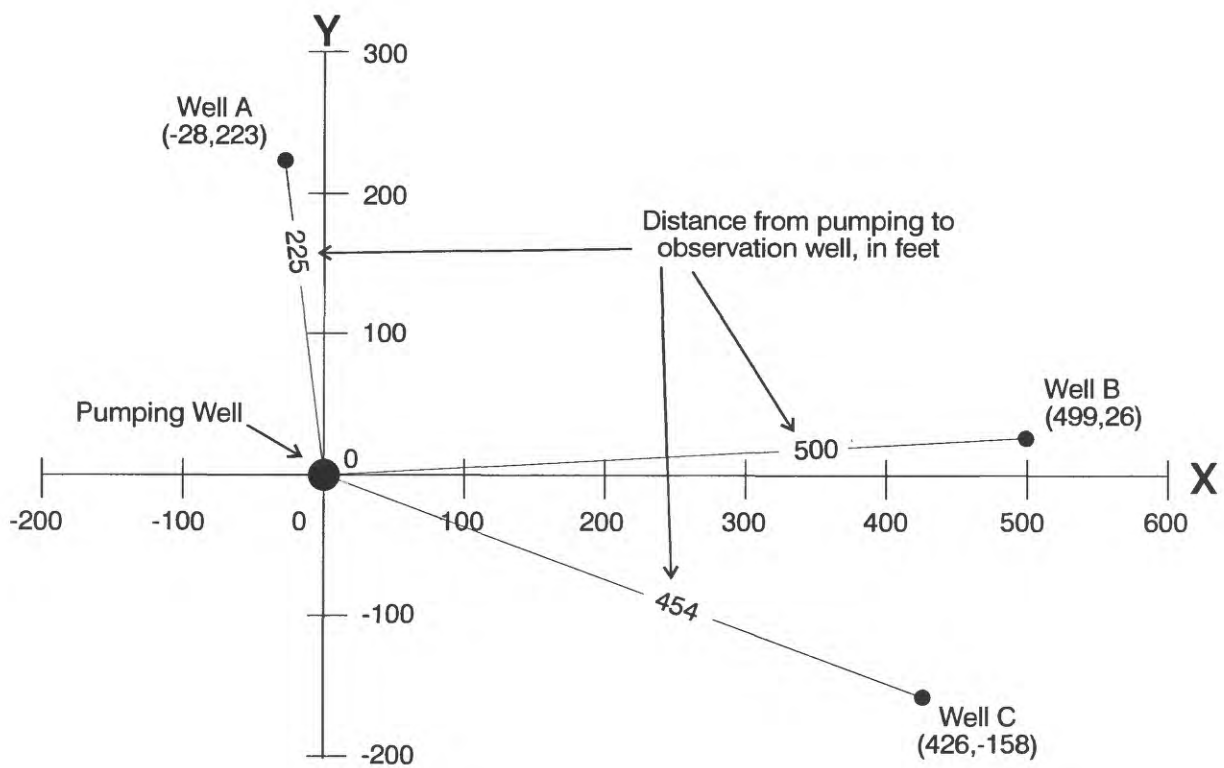


Figure 6.--Locations of observation wells in relation to the pumping well used in the aquifer test of the karst portion of the St. Peter-Prairie du Chien-Jordan aquifer conducted November 12, 1989 near Rochester, Minnesota, and generalized section of the pumping well.

the stream bed or within 50 ft of the stream, (2) presence of two or more straight (less than 30 degree curvature) segments of stream channel reach at least 500 ft in length, and (3) absence of tributaries. The stream channel reaches used to measure seepage are shown in figure 7.

Streamflow along reaches shown in figure 7 was measured with a current meter and by the radon method. Downstream gains or losses were calculated from differences in streamflow between upstream and downstream points. The rate of streamflow gain (or loss) per unit of stream channel length was the seepage rate. Streamflow changes measured with a current meter that were less than 10 percent are considered insignificant. The radon method is unable to measure downstream loss in streamflow; therefore, unless streamflow change determined by the radon method was a gain of at least 10 percent, the change was considered to be no gain.

The radon method is based on the generalization that activity of  $^{222}\text{Rn}$  in ground water ranges from two to four orders-of-magnitude greater than the  $^{222}\text{Rn}$  activity in surface water (King and others, 1982); therefore, seepage to streams generally increases the in-stream  $^{222}\text{Rn}$  activity. The calculation of the volume of seepage based on  $^{222}\text{Rn}$  activity uses a mass-balance equation that assumes insignificant loss of  $^{222}\text{Rn}$  to the atmosphere between two measuring points (Lee and Hollyday, 1987). The equation used to calculate seepage from in-stream measurements of  $^{222}\text{Rn}$  activities is

$$Q_{gw} = Q_m \times (A_m - A_s) / (A_{gw} - A_s)$$

where:

$Q_{gw}$  = rate of seepage,

$Q_m$  = rate of mixed stream/ground-water flow measured at downstream point,

$A_m$  = activity of  $^{222}\text{Rn}$  in mixed stream/ground-water at downstream point,

$A_s$  = activity of  $^{222}\text{Rn}$  in water at upstream point, and

$A_{gw}$  = activity of  $^{222}\text{Rn}$  in ground water from the Prairie du Chien Group.  $A_{gw}$  was determined from a measurement of the  $^{222}\text{Rn}$  activity in ground water discharged from the Prairie du Chien Group at a spring. This value of  $A_{gw}$  was assumed to be uniform for the study area because all of the seepage measured in this study was from the Prairie du Chien Group.

## Relation of Linear Terrain Features to Fracture Orientation

Land-surface features mapped as linear terrain features from aerial photographs are postulated to be indirect expressions of joints and fractures in the Prairie

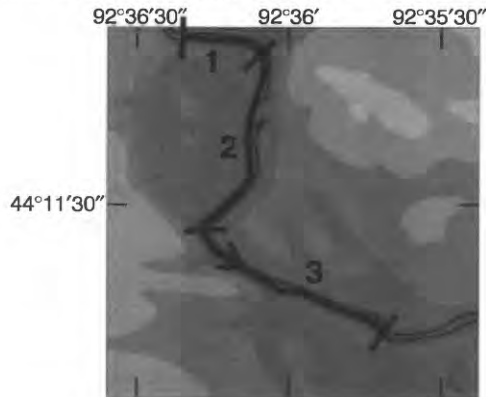
du Chien Group. This hypothesis was tested at 10 exposure sites by comparison of linear terrain features to fracture orientation measurements. Figures 8 through 17 contain pairs of rose diagrams constructed from fracture orientation data at the 10 sites and from linear terrain feature data in areas surrounding the sites. The diagrams show these data grouped by 30 degree increments. The chi square statistic and significance level for these data are shown in table 2. The null hypothesis tested by the chi square test is that the orientations of fractures and the directions of linear terrain features are randomly distributed among the arcs in the rose diagrams. A significance value less than 0.05 indicates a directional trend defined by at least one of the arcs.

The fracture orientations show statistically significant directionality at eight sites, and the linear terrain features show statistically significant directionality in areas that surround 4 of these 10 sites (table 2). Comparisons of the directional trends of the fractures to the linear terrain features where statistical analysis shows both sources of data exhibit directionality (sites 1, 3, and 10) indicate correlations at sites 1 and 10. The correlations for sites 1 and 10 are the arcs defined by an east-west line and a line N120°E, and an east-west line and a line N60°E, respectively (figs. 8 and 17). Results for sites 1 and 10 support the postulated relation between orientation of fractures and linear terrain features. The results for site 3, where the directional trends of the fracture orientation and linear terrain features lack correlation (fig. 10), do not support this postulated relation. Directional trends of fractures are statistically significant at five sites (sites 2, 5, 7, 8, and 9) where directional trends of the linear terrain features are not statistically significant. Directional trends of the linear terrain features are statistically significant at one site (site 4) where directional trends of the fractures are not statistically significant. The results for sites 2, 4, 5, 7, 8, and 9 are inconsistent with the postulated relation between linear terrain features and fractures. Therefore orientation of linear terrain features is not a reliable indicator of fracture orientation in the Prairie du Chien Group of southeastern Minnesota except possibly where these features show statistically significant directional trends.

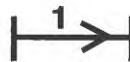
## Relation of Anisotropy of Transmissivity to Fracture Orientation

Aquifer-test results indicate that the Prairie du Chien Group is anisotropic at the test site. Log-log plots of the drawdown versus the ratio of time from the start of

### A. Middle Fork of Zumbro River



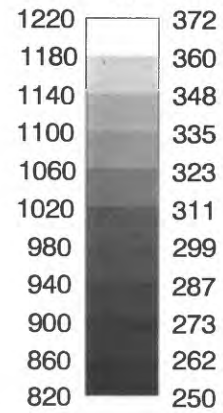
### EXPLANATION

 Stream reach. Number designates stream reach. Arrows indicate direction of streamflow. Lines across stream channel bracket upstream and downstream ends of reach.

 River shoreline

Elevation above sea level

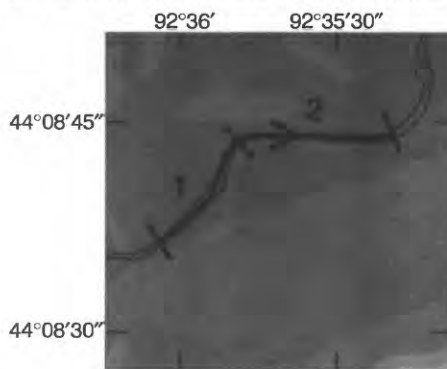
### FEET METERS



Base from U.S. Geological Survey digital data, 1:24,000, 1965, 1972, Universal Transverse Mercator Projection, Zone 15



### B. South Branch of Middle Fork of Zumbro River



### C. South Branch of Root River

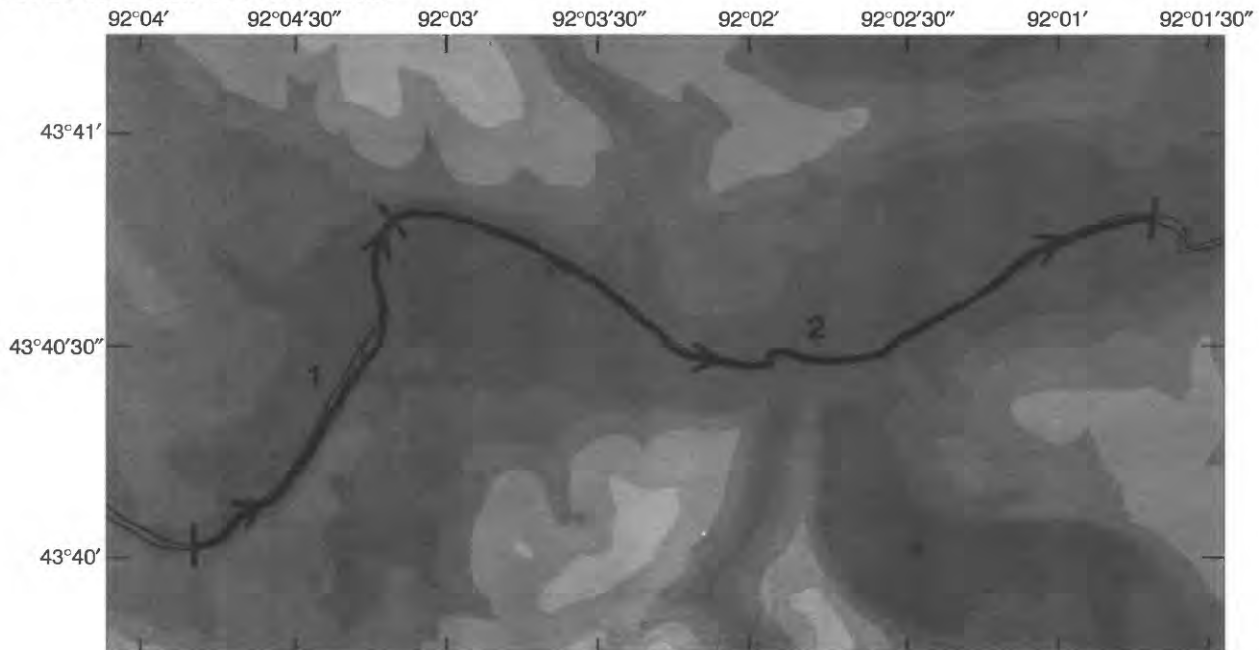
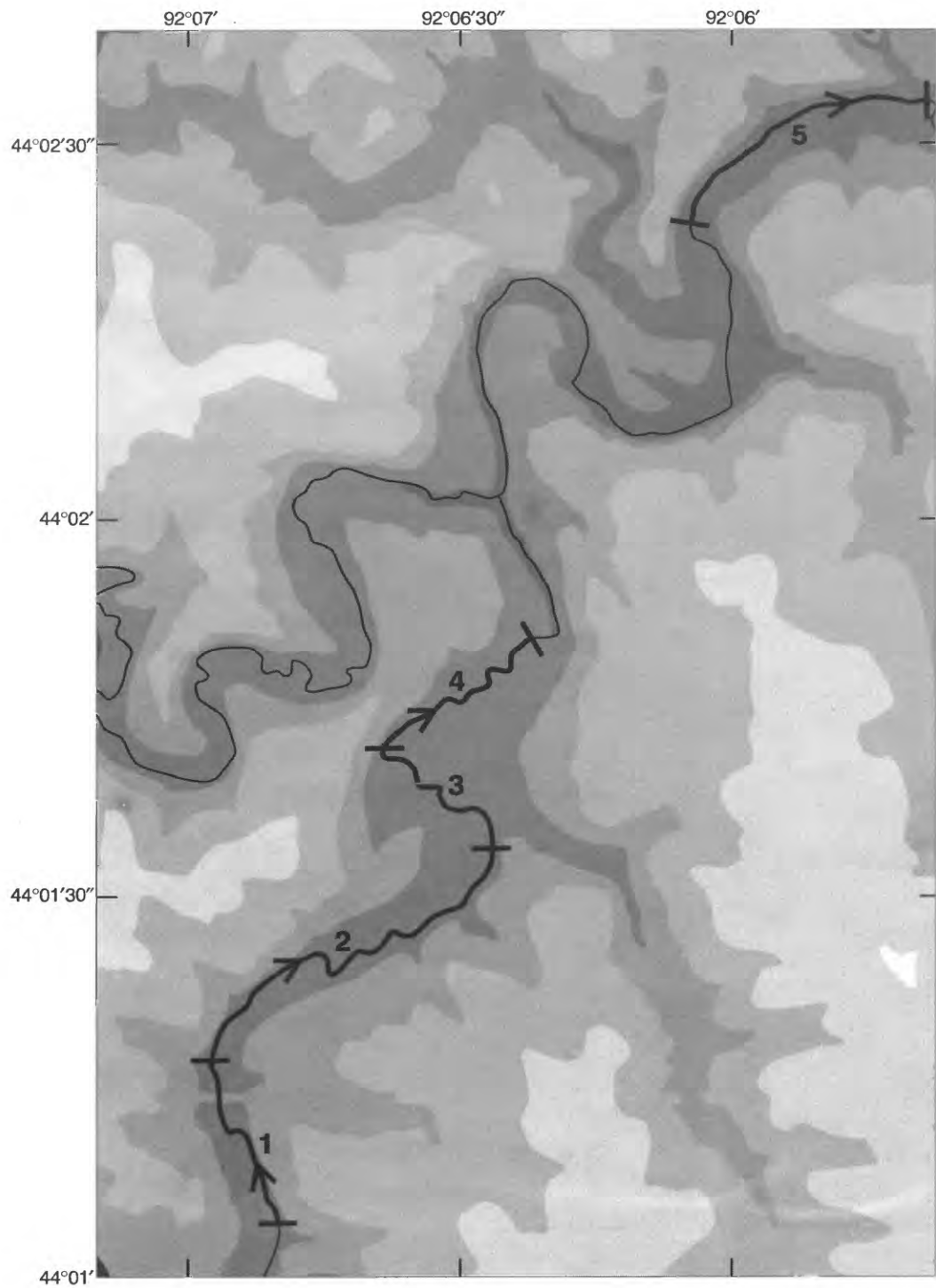


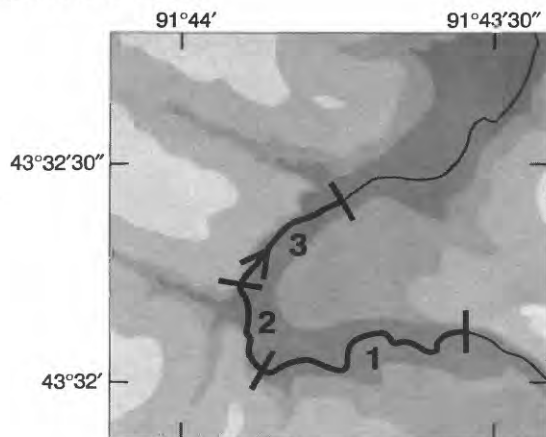
Figure 7a.--Stream channel reaches used to measure seepage rates

**D. Crow Creek and Middle Fork of Whitewater River**

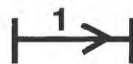


at four seepage-measurement sites in southeastern Minnesota.

### E. Riceford Creek



### EXPLANATION



Stream reach. Number designates stream reach. Arrows indicate direction of streamflow. Lines across stream channel bracket upstream and downstream ends of reach.



River shoreline

Base from U.S. Geological Survey digital data, 1:24,000, 1965, Universal Transverse Mercator Projection, Zone 15

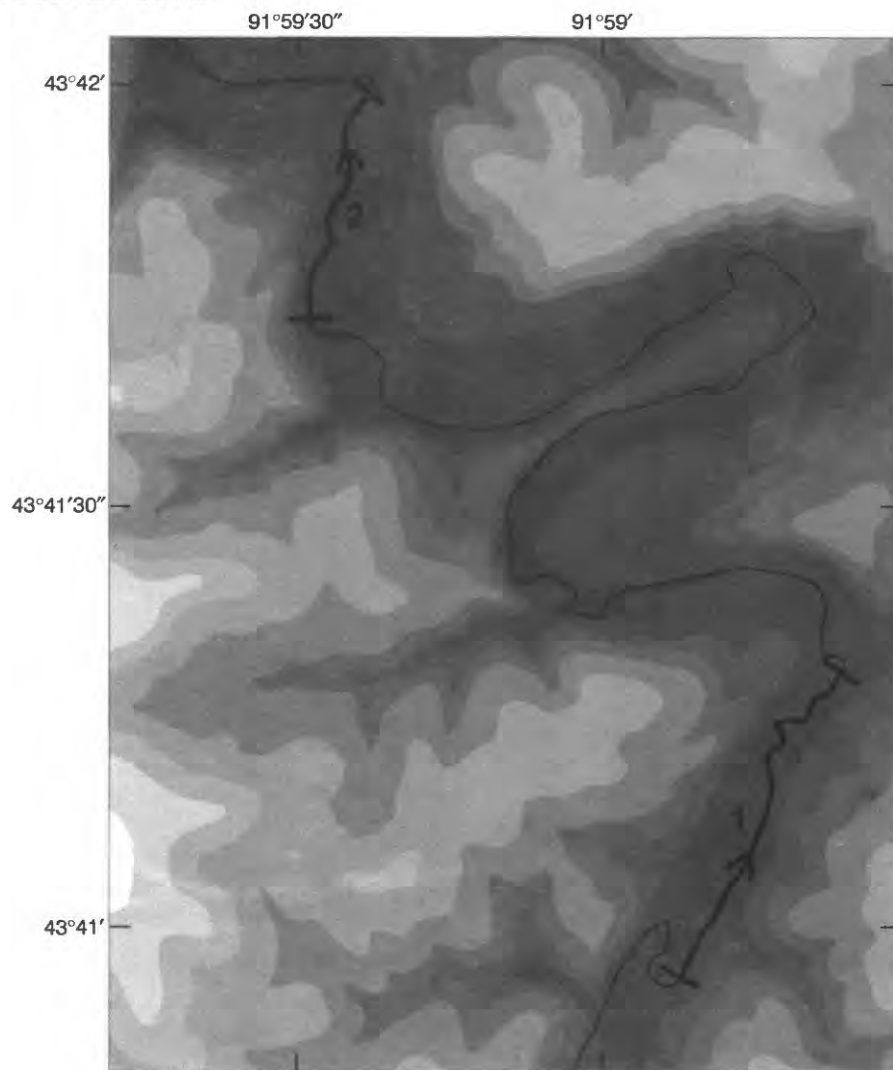
Elevation above sea level

**FEET METERS**

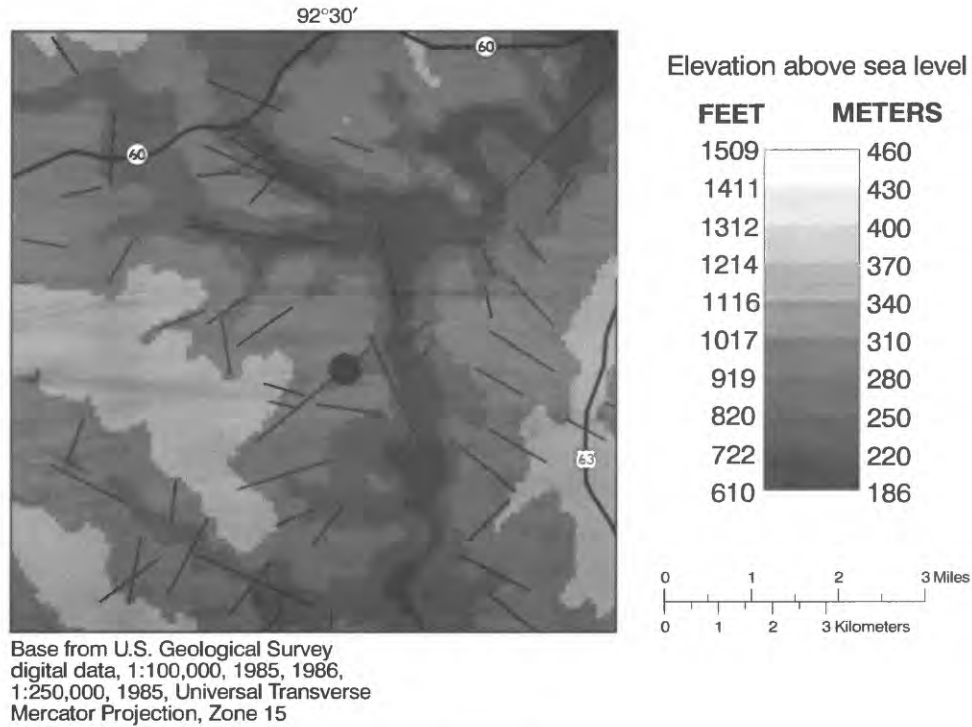
1220	372
1180	360
1140	348
1100	335
1060	323
1020	311
980	299
940	287
900	273
860	262
820	250

0 0.1 0.2 0.3 0.4 Miles

### F. Duschee Creek



**Figure 7b.--Stream channel reaches used to measure seepage rates at two seepage measurement sites in southeastern Minnesota.**

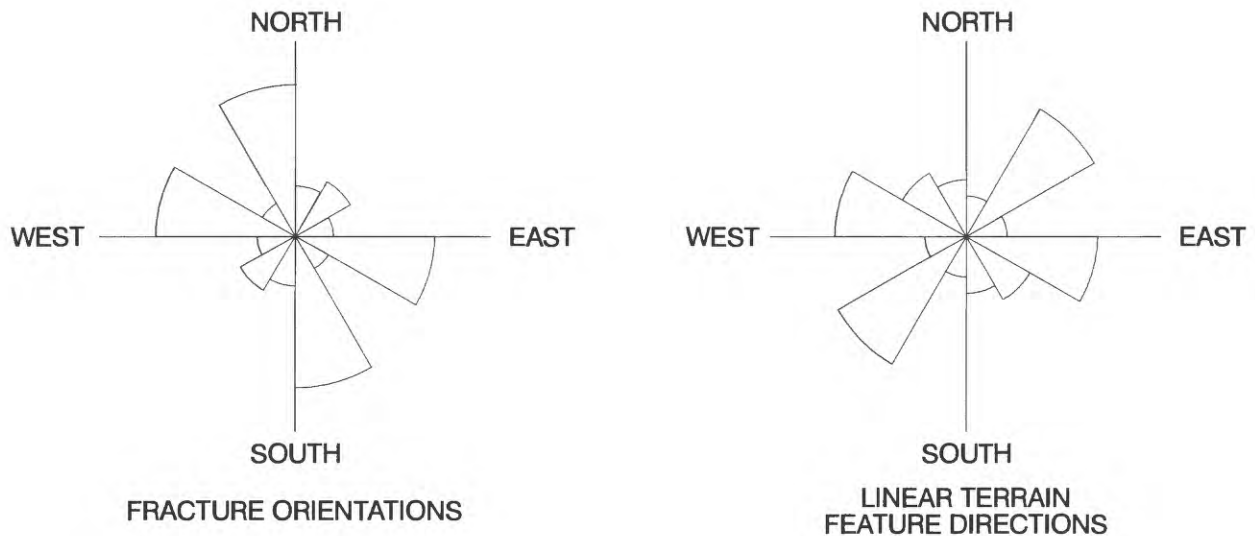


**EXPLANATION**

— Linear terrain feature

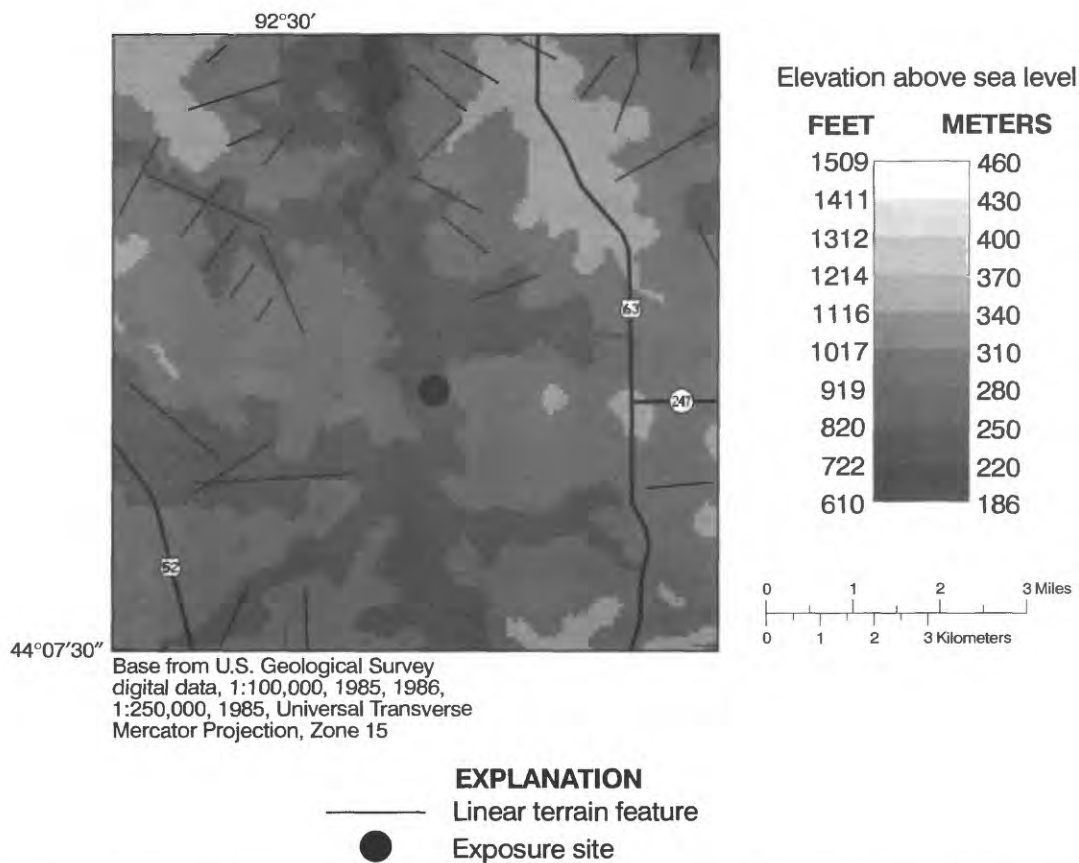
● Exposure site

A. Linear terrain features in area surrounding exposure site 1, Sec. 10, T.109N., R.14W.

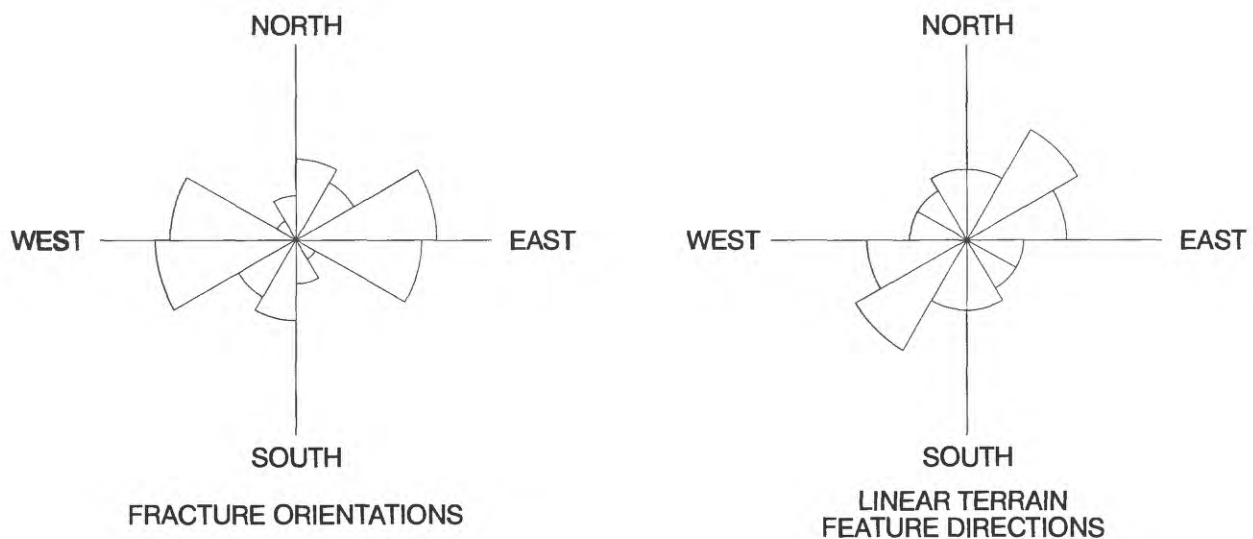


B. Rose diagrams of fracture orientations and of linear terrain features for exposure site 1. Radial length of petals is proportional to number of observations within the petal.

**Figure 8.--Map of linear terrain features and rose diagrams of these features and of fracture orientation measurements for exposure site 1 of the Prairie du Chien Group in southeastern Minnesota.**

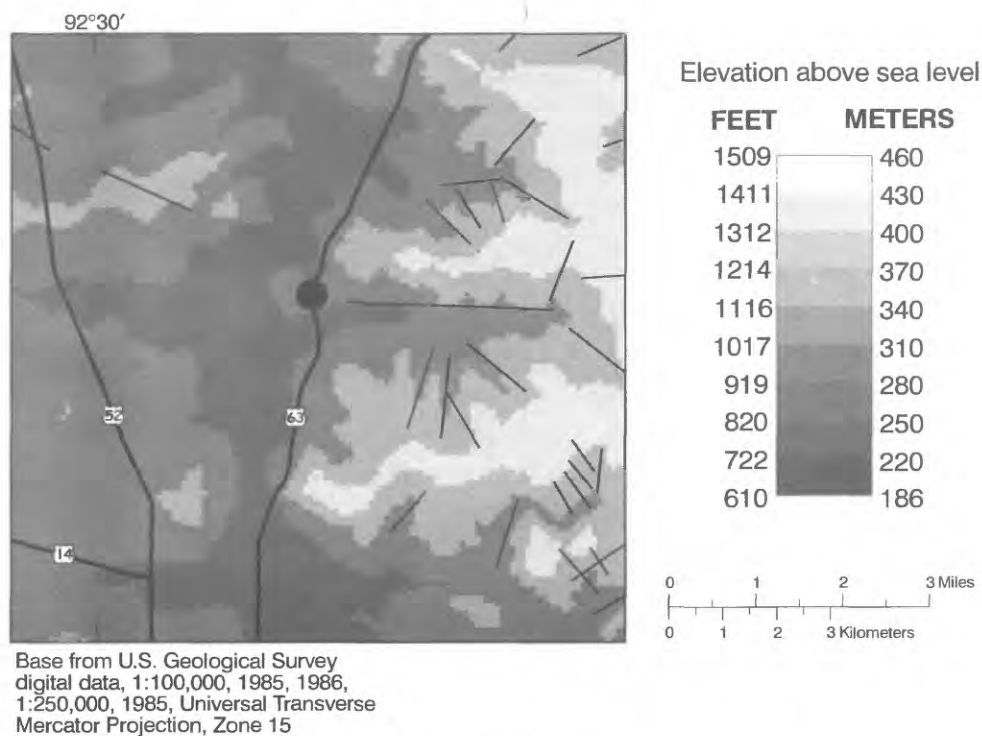


A. Linear terrain features in area surrounding exposure site 2, Sec. 11, T.108N., R.14W.

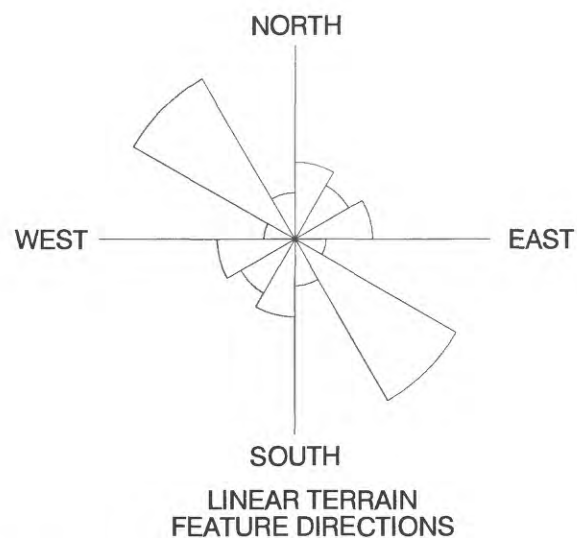
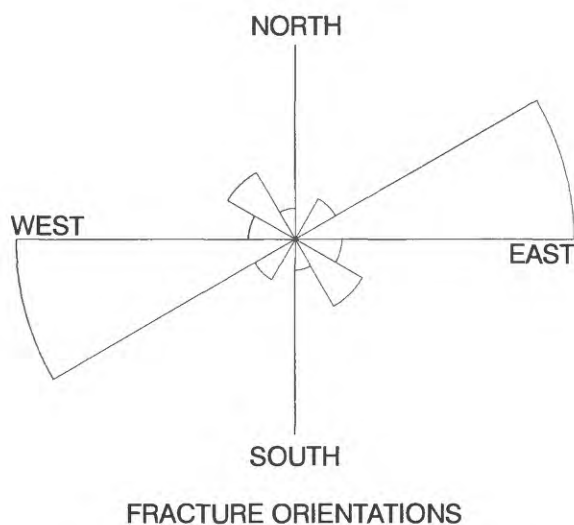


B. Rose diagrams of fracture orientations and of linear terrain features for exposure site 2. Radial length of petals is proportional to number of observations within the petal.

**Figure 9.--Map of linear terrain features and rose diagrams of these features and of fracture orientation measurements for exposure site 2 of the Prairie du Chien Group in southeastern Minnesota.**

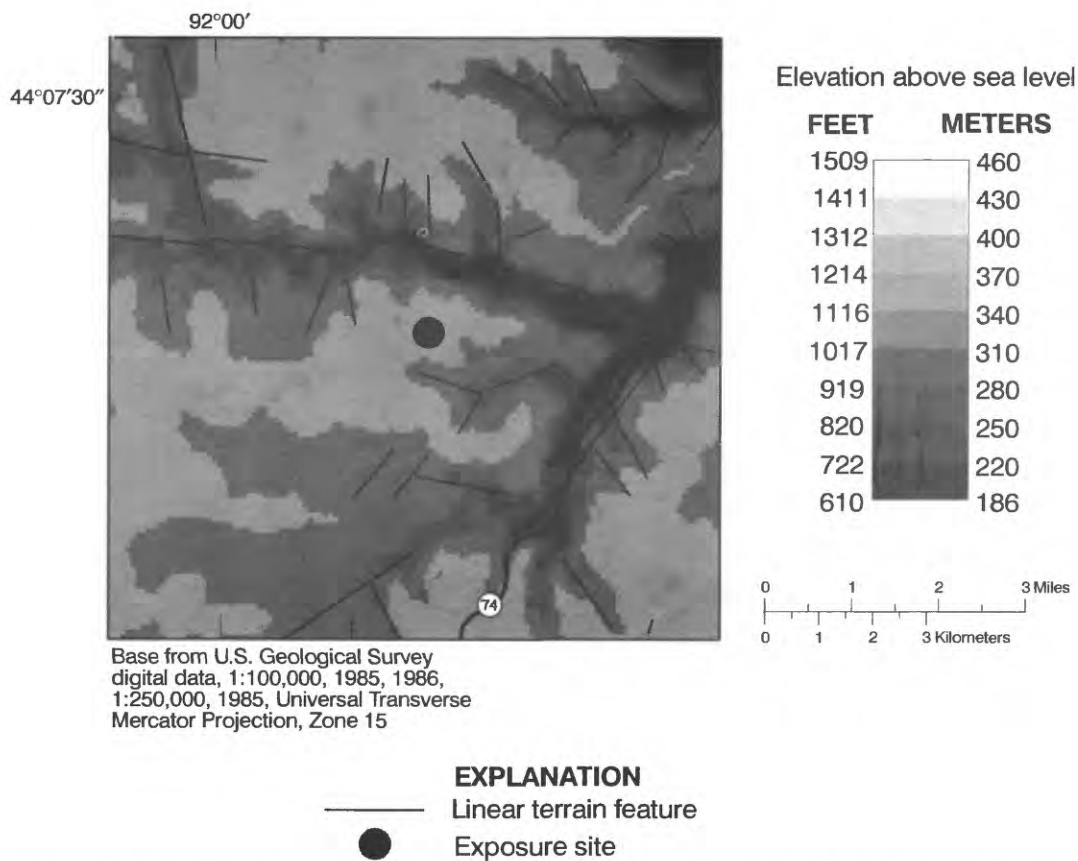


A. Linear terrain features in area surrounding exposure site 3, Sec. 14, T.107N., R.14W.

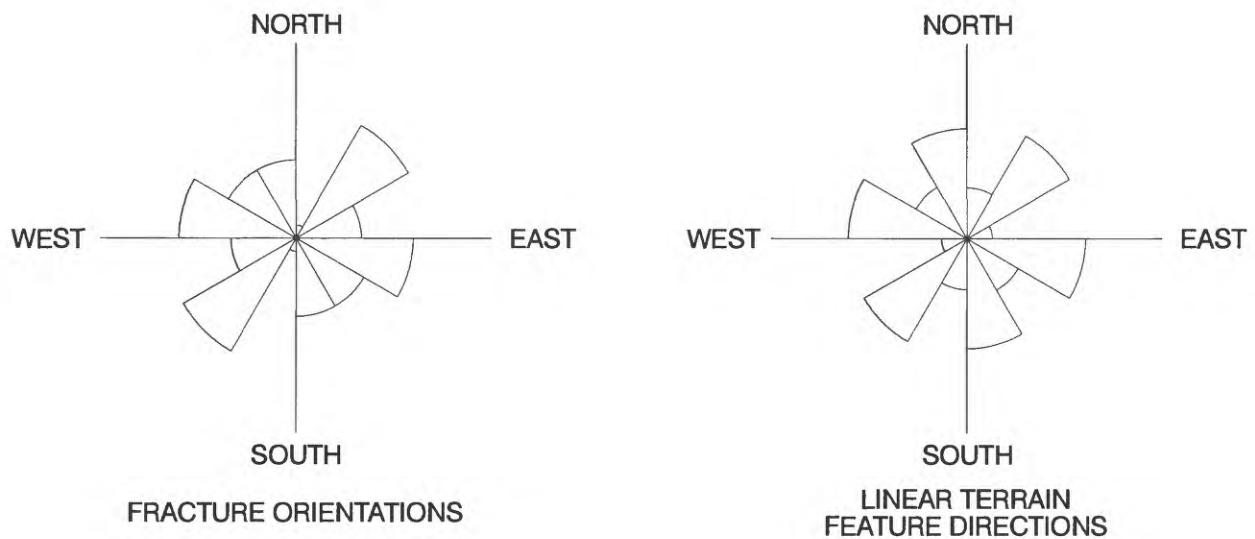


B. Rose diagrams of fracture orientations and of linear terrain features for exposure site 3. Radial length of petals is proportional to number of observations within the petal.

**Figure 10.--Map of linear terrain features and rose diagrams of these features and of fracture orientation measurements for exposure site 3 of the Prairie du Chien Group in southeastern Minnesota.**

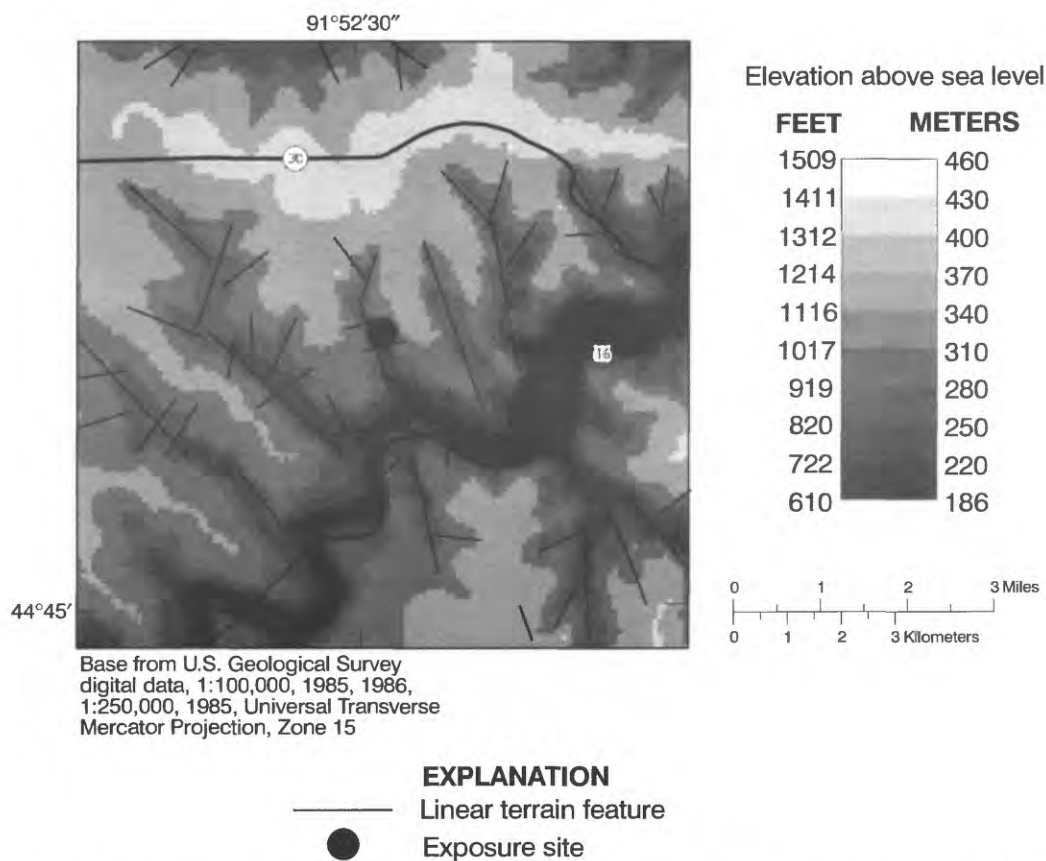


A. Linear terrain features in area surrounding exposure site 4, Sec. 7, T.107N., R.09W.

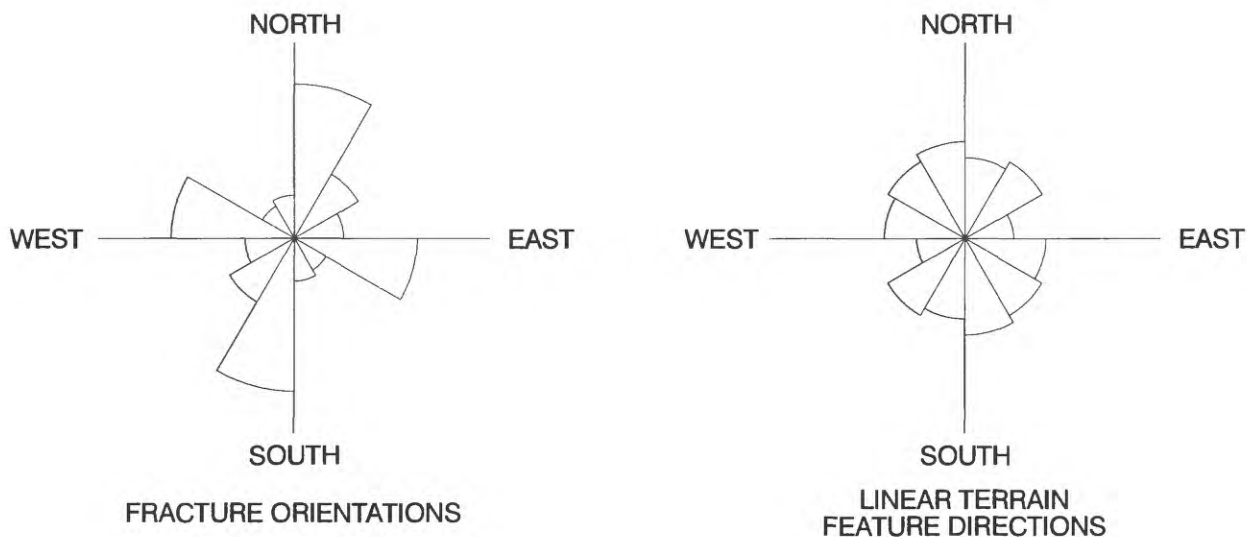


B. Rose diagrams of fracture orientations and of linear terrain features for exposure site 4. Radial length of petals is proportional to number of observations within the petal.

**Figure 11.--Map of linear terrain features and rose diagrams of these features and of fracture orientation measurements for exposure site 4 of the Prairie du Chien Group in southeastern Minnesota.**

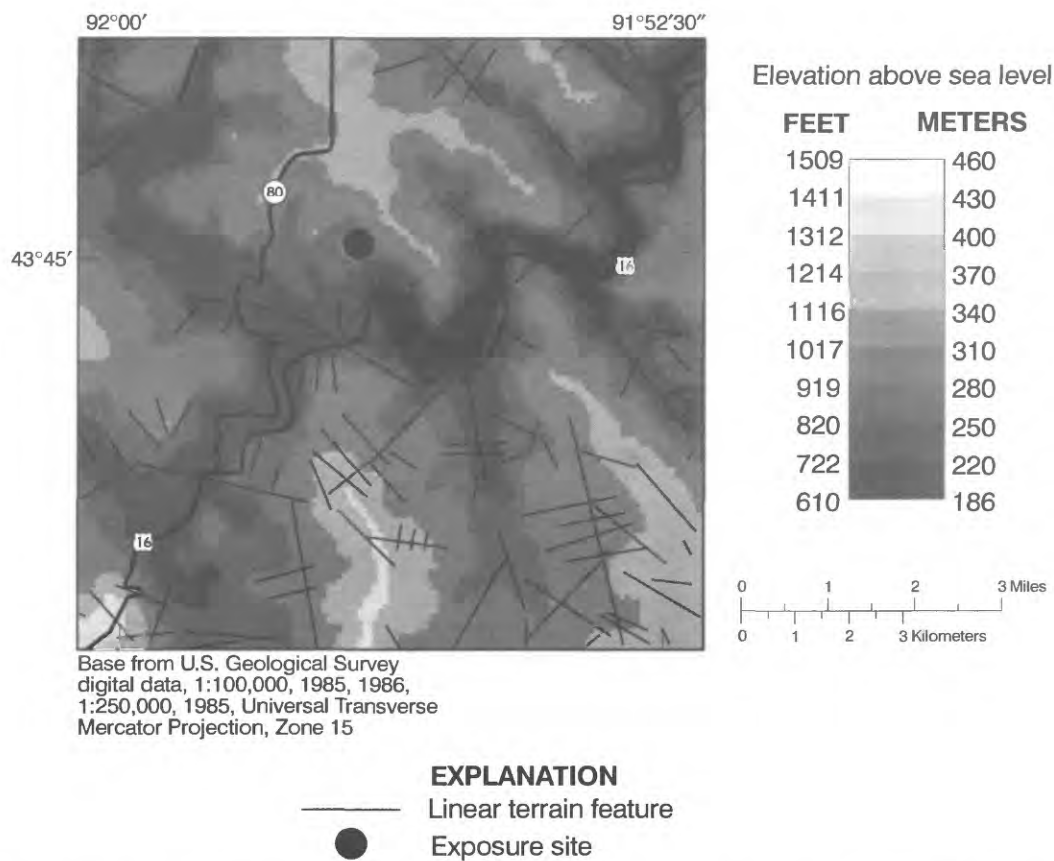


A. Linear terrain features in area surrounding exposure site 5, Sec. 25, T.104N., R.09W.

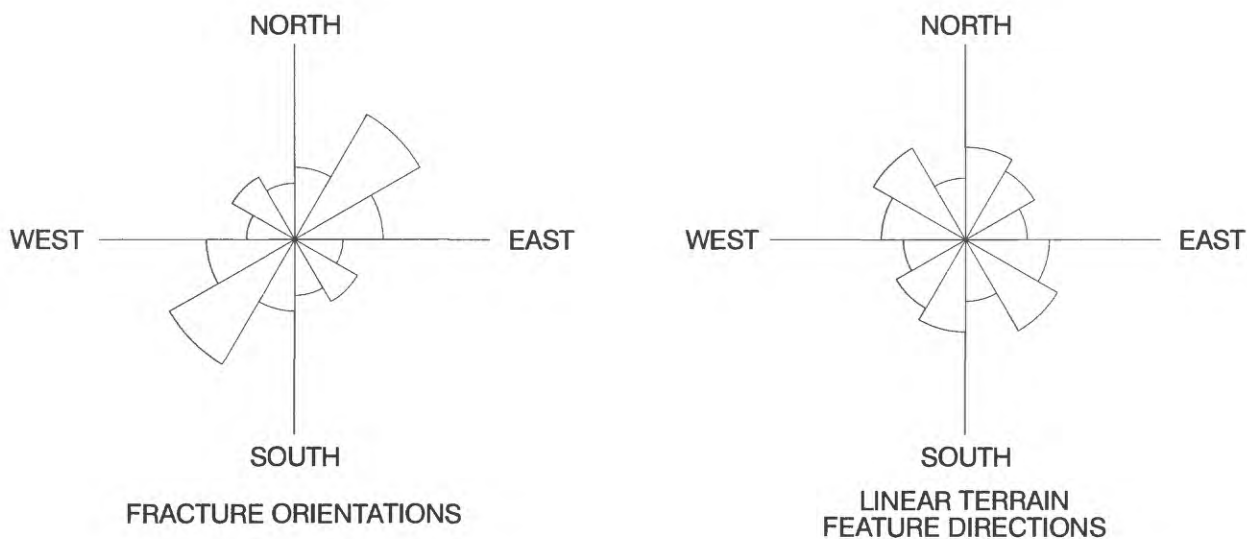


B. Rose diagrams of fracture orientations and of linear terrain features for exposure site 5. Radial length of petals is proportional to number of observations within the petal.

**Figure 12.--Map of linear terrain features and rose diagrams of these features and of fracture orientation measurements for exposure site 5 of the Prairie du Chien Group in southeastern Minnesota.**

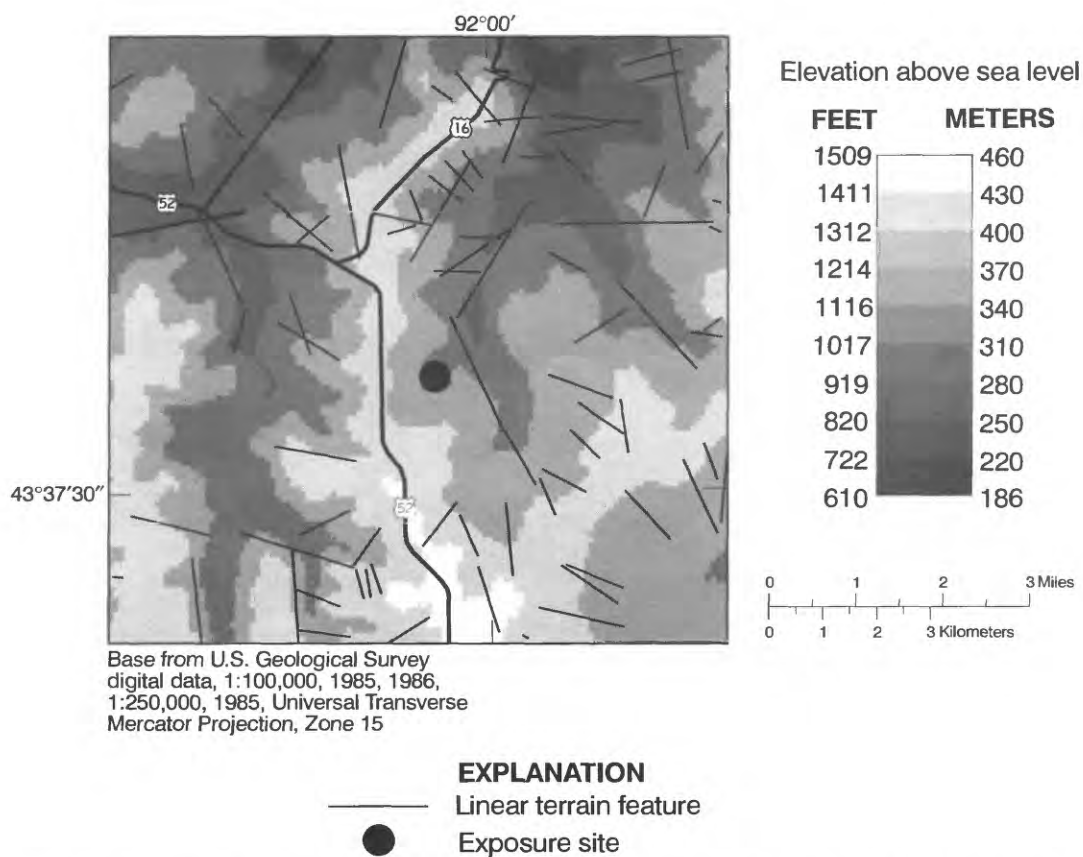


A. Linear terrain features in area surrounding exposure site 6, Sec. 8, T.103N., R.09W.

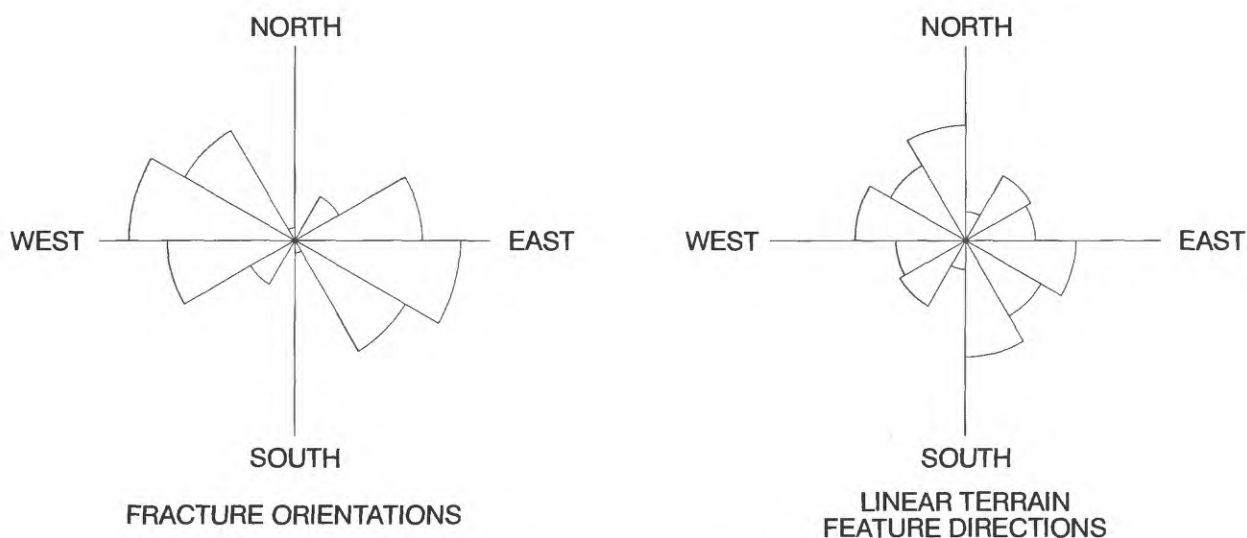


B. Rose diagrams of fracture orientations and of linear terrain features for exposure site 6. Radial length of petals is proportional to number of observations within the petal.

**Figure 13.--Map of linear terrain features and rose diagrams of these features and of fracture orientation measurements for exposure site 6 of the Prairie du Chien Group in southeastern Minnesota.**

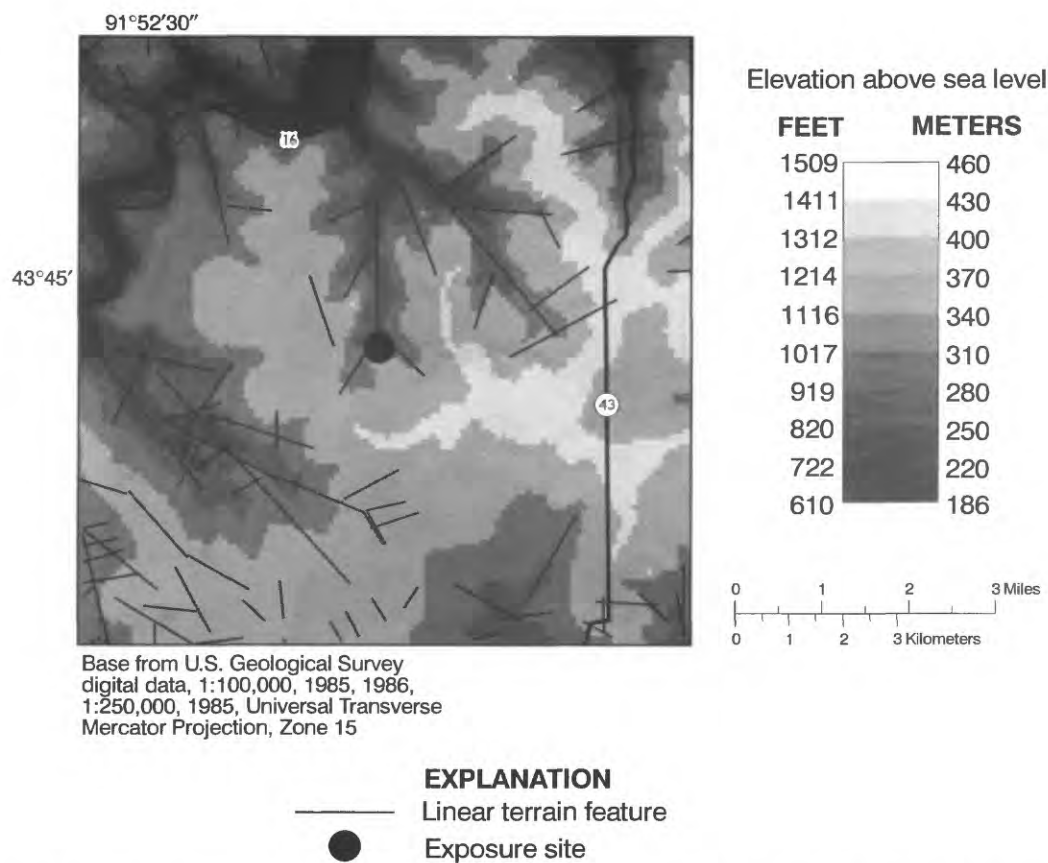


A. Linear terrain features in area surrounding exposure site 7, Sec. 7, T.102N., R.09W.

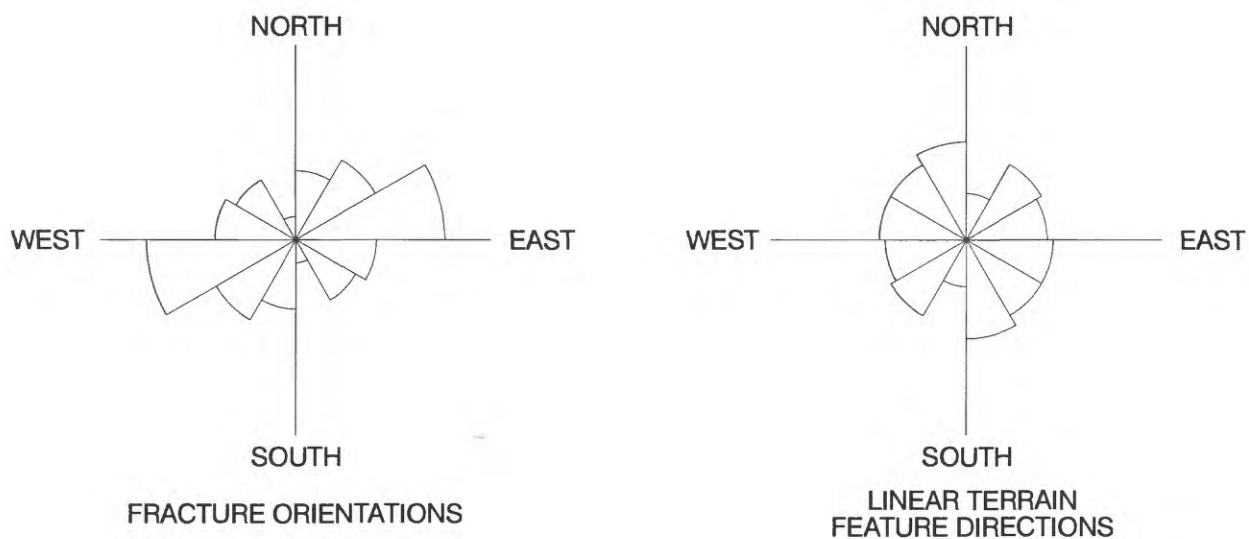


B. Rose diagrams of fracture orientations and of linear terrain features for exposure site 7. Radial length of petals is proportional to number of observations within the petal.

**Figure 14.--Map of linear terrain features and rose diagrams of these features and of fracture orientation measurements for exposure site 7 of the Prairie du Chien Group in southeastern Minnesota.**

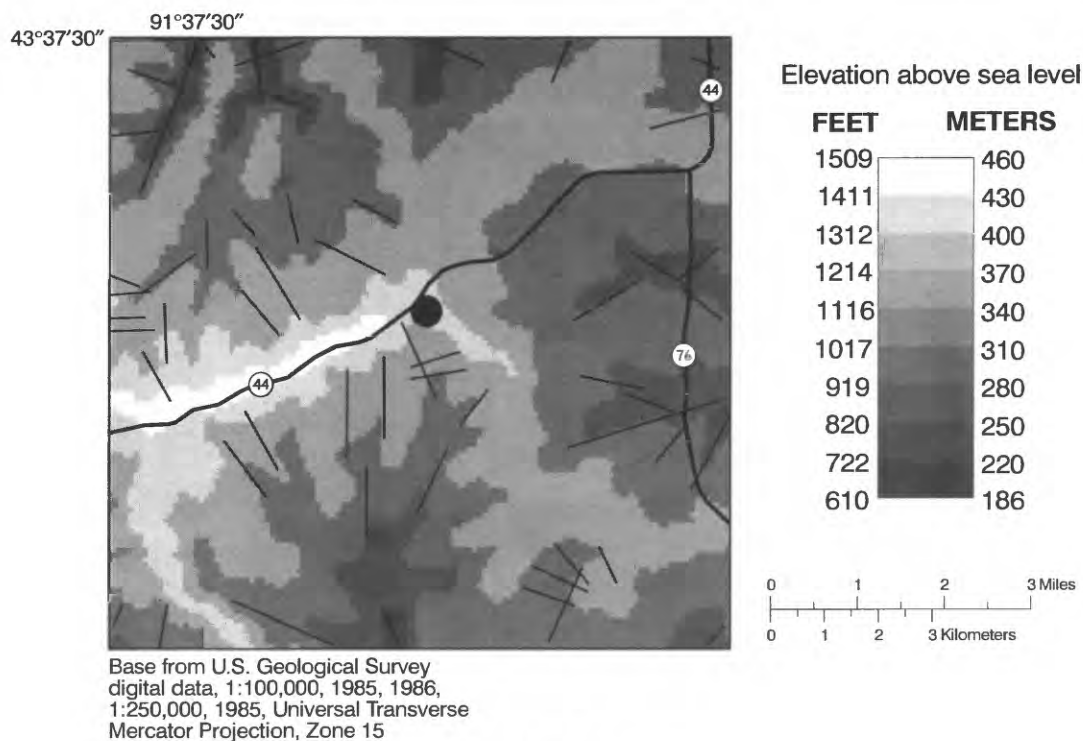


A. Linear terrain features in area surrounding exposure site 8, Sec. 8, T.103N., R.08W.

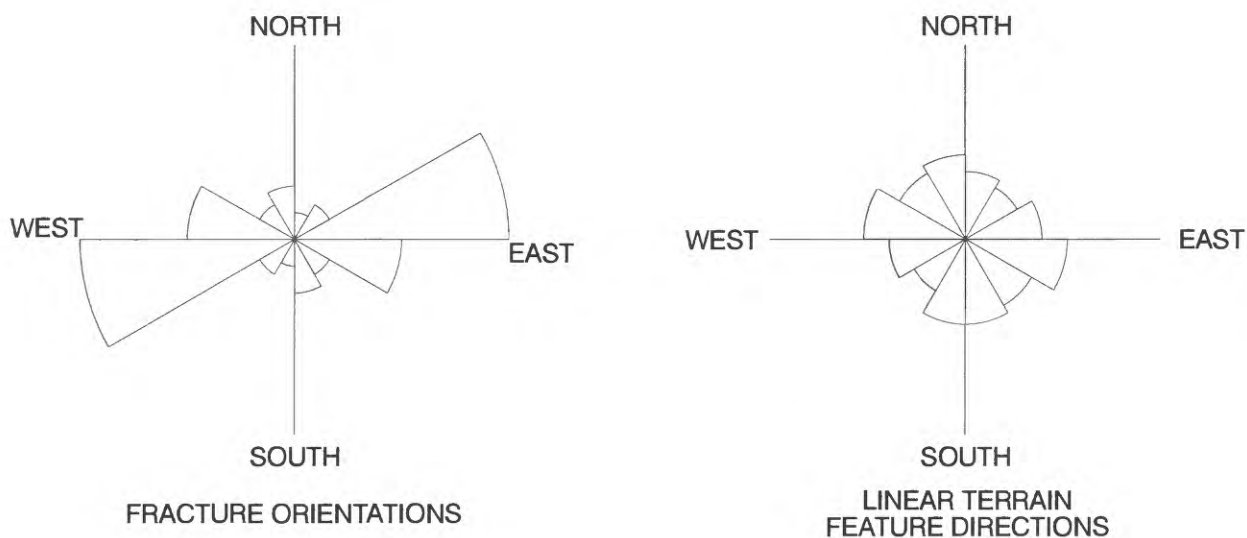


B. Rose diagrams of fracture orientations and of linear terrain features for exposure site 1. Radial length of petals is proportional to number of observations within the petal.

**Figure 15.—Map of linear terrain features and rose diagrams of these features and of fracture orientation measurements for exposure site 8 of the Prairie du Chien Group in southeastern Minnesota.**

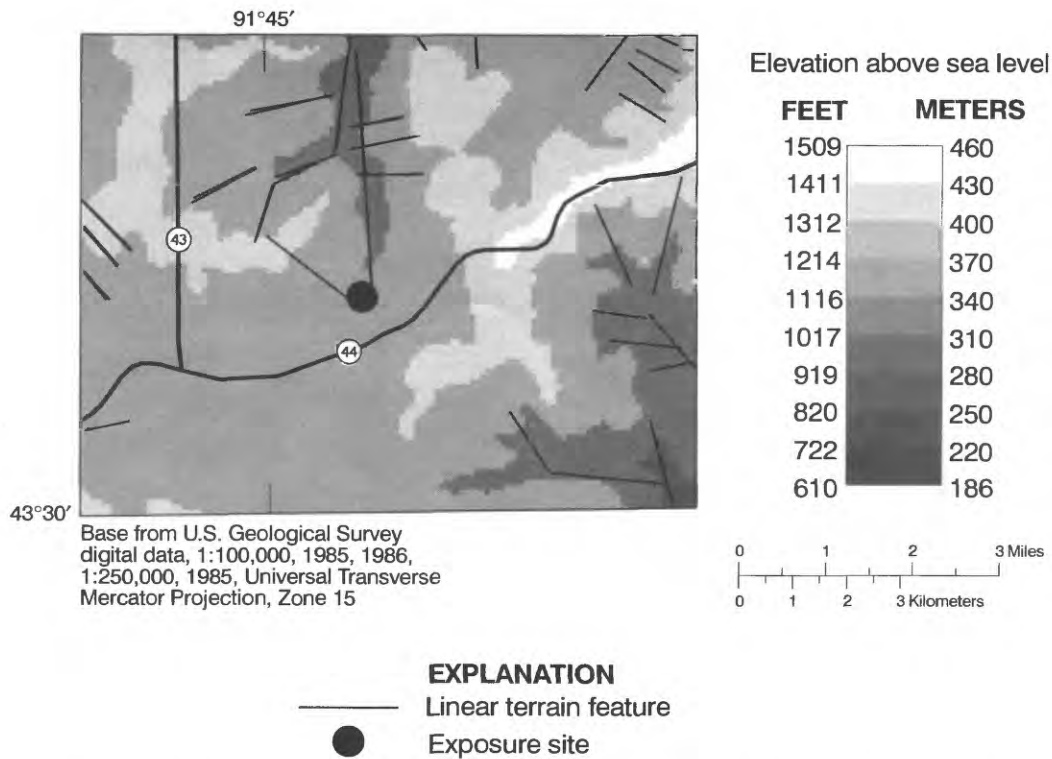


A. Linear terrain features in area surrounding exposure site 9, Sec. 5, T.101N., R.06W.

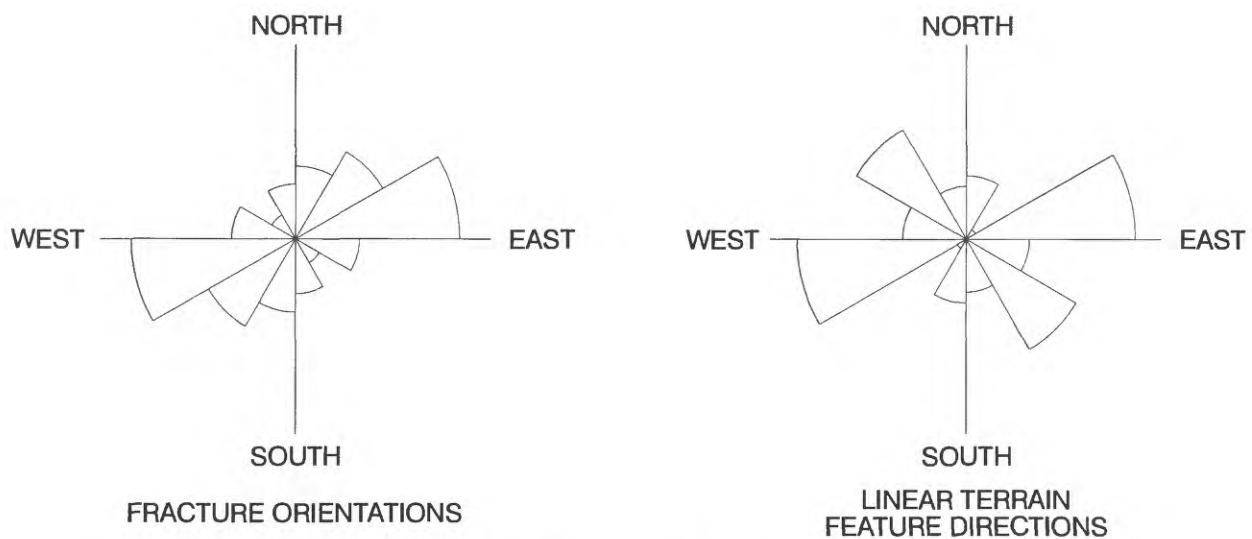


B. Rose diagrams of fracture orientations and of linear terrain features for exposure site 9. Radial length of petals is proportional to number of observations within the petal.

**Figure 16.--Map of linear terrain features and rose diagrams of these features and of fracture orientation measurements for exposure site 9 of the Prairie du Chien Group in southeastern Minnesota.**



A. Linear terrain features in area surrounding exposure site 10, Sec. 19, T.101N., R.07W.



B. Rose diagrams of fracture orientations and of linear terrain features for exposure site 10. Radial length of petals is proportional to number of observations within the petal.

**Figure 17.--Map of linear terrain features and rose diagrams of these features and of fracture orientation measurements for exposure site 10 of the Prairie du Chien Group in southeastern Minnesota.**

Table 1.--Seepage rates along stream reaches at six sites

[ft, feet; ft<sup>3</sup>/s, cubic feet per second; dpm/L, disintegrations per minute per liter; N.S.C., no significant change (less than 0.10); N.G., no gain; --, no data; activity of <sup>222</sup>Rn in ground water used to calculate seepage rates is 410 dpm/L]

Stream	Date	Reach	Seepage measurement site (shown on figure 5)	Measured streamflow (ft <sup>3</sup> /s)			Seepage rate expressed as change in streamflow per 1,000 lineal feet of stream channel (ft <sup>3</sup> /s/1,000 ft)			
				Length of reach (ft)	Upstream part of reach	Downstream part of reach	Upstream radon activity (dpm/L)	Downstream radon activity (dpm/L)	Current meter measurement	Radon method
Middle Fork Zumbro River	8/29/88	1	A	700	6.5	6.4	--	--	N.S.C.	--
	8/29/88	2		1,325	6.4	6.5	80.7	74.1	N.S.C.	N.G.
	8/29/88	3		1,325	6.5	6.7	74.1	80.7	N.S.C.	.10
South Branch of the Middle Fork of the Zumbro River	8/29/88	1	B	1,000	12.3	10.8	130	87	-1.50	N.G.
	8/29/88	2		1,175	10.8	11.1	87.6	102	N.S.C.	.42
Crow Creek	8/29/88	1	C	1,500	6.0	7.3	138	193	.87	.98
	8/29/88	2		2,650	7.3	7.1	--	--	N.S.C.	--
	8/29/88	3		1,325	7.1	8.3	--	--	.15	--
	8/29/88	4		1,500	8.3	7.1	71.8	56.3	-.80	N.G.
Middle Fork Whitewater River	8/30/88	5		2,000	9.8	10.6	89.8	102	N.S.C.	.20
South Branch Root River	8/30/88	1	D	2,750	28.4	27.1	125	126	N.S.C.	N.G.
	8/30/88	2		5,500	27.1	43.5	95.8	103	2.98	.18
Duschee Creek	8/31/88	1	E	2,325	6.8	6.6	59.8	58.1	N.S.C.	N.G.
	8/31/88	2		1,800	7.5	8.5	141	171	.55	.53
Riceford Creek	8/31/88	1	F	1,500	1.4	1.7	62.8	95.5	.20	.33
	8/31/88	2		650	1.7	2.2	165	216	.77	.70
	8/31/88	3		650	2.2	2.5	216	333	.46	2.32

Table 2.--Chi square statistic computed for fracture orientations at ten exposure sites in the Prairie du Chien Group and for linear terrain features interpreted from aerial photographs of areas shown in figures 8 through 17 that surround the exposure sites

[F, fracture measurements; L, linear terrain features; site numbers correspond to site index numbers shown in figure 3; N, number of observations;  $X^2$ , chi square statistic; Significance is the probability that rejection of the null hypothesis, which is that the arcs of the rose diagrams in figures 8 through 17 have no directional trends, is in error. A significance value less than 0.0500 indicates rejection of the null hypothesis.]

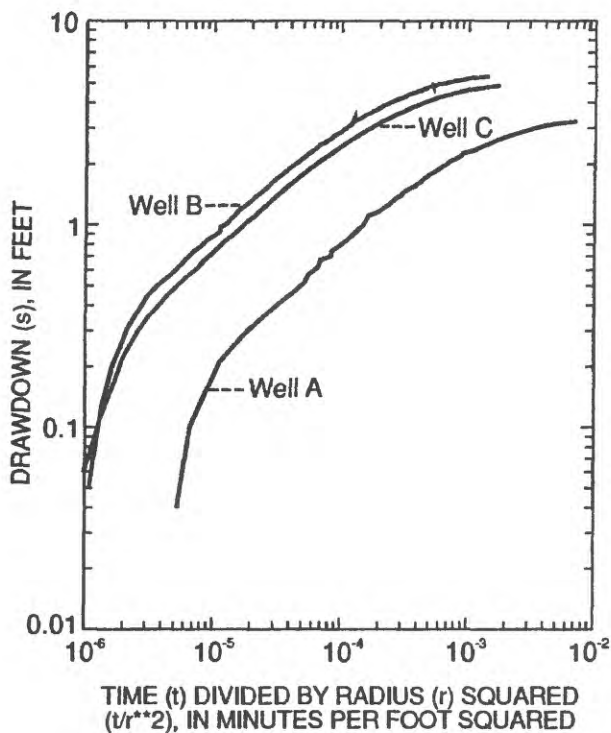
Site number and type	N	$X^2$	Significance
1 F	38	13.158	0.0219
L	60	16.000	.0068
2 F	65	17.800	.0032
L	34	3.412	.6368
3 F	31	40.807	.0000
L	31	12.161	.0326
4 F	37	8.243	.1433
L	57	11.947	.0355
5 F	78	23.385	.0003
L	60	2.200	.8208
6 F	60	9.200	.1013
L	110	4.218	.5184
7 F	38	22.947	.0004
L	84	10.571	.0606
8 F	42	16.000	.0138
L	84	3.429	.6342
9 F	36	23.667	.0003
L	55	1.6182	.8990
10 F	53	15.264	.0093
L	46	18.956	.0020

pumping to the square of the distance between the pumping well and observation wells indicate that the water-level decline was greatest in well B and was smallest in well A (fig. 18). Match point coordinates for  $[W(\mu)+\bar{f}]$ ,  $\mu$ , drawdown ( $s$ ), and time ( $t$ ) were determined for each of the three observation wells by a curve-matching method (fig. 19). The plots of drawdown versus time in figure 19 indicate that the pumping rate (240 gal/min) of the production well decreased slightly from about one minute to about five minutes after the test began. Analyses of the aquifer-test data by the methods documented by Maslia and Randolph (1987) indicate that the axis of major horizontal transmissivity of 8,974 ft<sup>2</sup>/d is oriented

N95°E and that the axis of minor horizontal transmissivity of 1,788 ft<sup>2</sup>/d is oriented N5°E. The storage coefficient determined from this analysis is  $1.056 \times 10^{-4}$ . These results indicate that at the aquifer-test site the major axis of joint fractures in the Prairie du Chien Group is slightly clockwise from east to west.

### Relation of Linear Terrain Features to Seepage

This study assumes that seepage from the karst portion of the St. Peter-Prairie du Chien-Jordan aquifer to streams is (1) greatest where the major axes of linear terrain features are perpendicular to the stream reaches,



**Figure 18.--Drawdown at each of three observation wells during pumping of a production well at 240 gallons per minute for an aquifer test of the St. Peter-Prairie du Chien-Jordan aquifer conducted November 12, 1989, near Rochester, Minnesota.**

and (2) is smallest where the minor axes of linear terrain features are perpendicular to the stream reaches.

The relation of the directional trends of linear terrain features to seepage from the Prairie du Chien Group was analyzed along stream reaches (fig. 7) at the six seepage-measurement sites shown in figure 5. Seepage rates ranged from stream losses of 1.5 ft<sup>3</sup>/s per 1,000 ft of channel to stream gains of 2.98 ft<sup>3</sup>/s per 1,000 ft of channel (table 1). Seepage rates estimated by the radon method were within 65 percent of values obtained by current-meter measurements except along reach 3 in Riceford Creek, reach 2 of the South Branch of the Middle Fork of the Zumbro River, and reach 2 of the South Branch of the Root River (table 1). The radon method does not estimate streamflow loss, thus, the absence of any gain estimated by the radon method for reach 1 of the South Branch of the Zumbro River and for reach 4 of the Crow River are consistent with the loss of streamflow determined by the current meter method.

One possible explanation for the low seepage rate from the radon technique in reach 2 along the South Branch of the Root River is that a significant amount of <sup>222</sup>Rn escaped from the stream as gas between the

upstream and downstream sampling points and lowered the <sup>222</sup>Rn activity in the downstream sample. Riffles under a bridge located about midway between the upstream and downstream sampling points of this reach were a possible cause of accelerated <sup>222</sup>Rn loss.

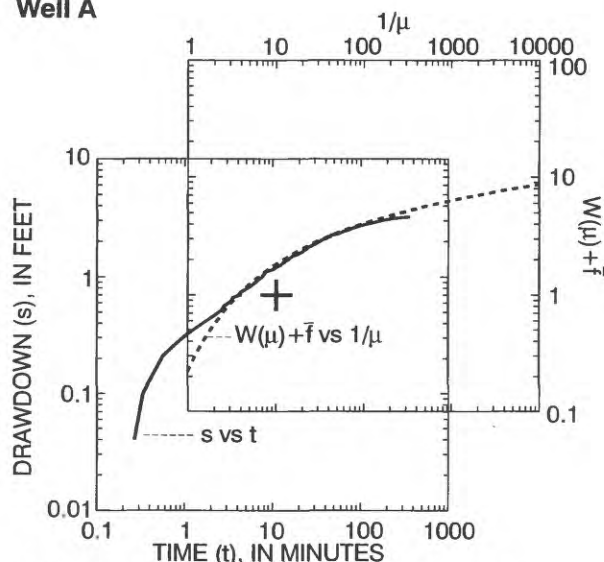
Linear terrain features delineated in the areas surrounding the seepage-measurement sites are shown in figures 20 through 25. Rose diagrams show the directional trends of the linear terrain features and the direction of the stream channels. Table 3 shows the results of chi square tests performed to determine the statistical significance of the directional trends. A significance value less than 0.05 indicates a directional trend defined by at least one of the arcs of the rose diagram.

The linear terrain features do not show statistically significant directional trends in the areas surrounding the Middle Fork of the Zumbro River, the South Branch of the Middle Fork of the Zumbro River, and the South Branch of the Root River (table 3). Therefore, the hypotheses of the study cannot be tested at these sites. The linear terrain features do show statistically significant trends in the areas surrounding Crow Creek and the Middle Fork of the Whitewater River, Duscree Creek, and Riceford Creek (table 3). The hypotheses of the study can be tested at these three sites.

The dominant directional trend of linear terrain features in the area surrounding Crow Creek and the Middle Fork of the Whitewater River is within an arc defined by a north-south line and a line N150°E (fig. 22b). The largest seepage rate was in reach 1, which is approximately aligned with the dominant direction of local linear terrain features (fig. 22b). The second and third largest seepage rates were in reaches 4 and 5, respectively, which are approximately aligned with the minor direction of local linear terrain features. Reach 2 is aligned in approximately the same direction as reach 4. The seepage rates for reaches 2 and 3 were small. The study hypotheses predict maximum seepage in reaches 2, 4 and 5. These three reaches are at an angle of about 90 degrees to the dominant direction of local linear terrain features. The study hypotheses also predict minimum seepage in reaches 1 and 3 because reach 1 is approximately aligned with, and reach 3 is nearly aligned with, the dominant direction of local linear terrain features. The results for reaches 3, 4 and 5 are consistent with the hypotheses, and the results for reaches 1 and 2 are inconsistent.

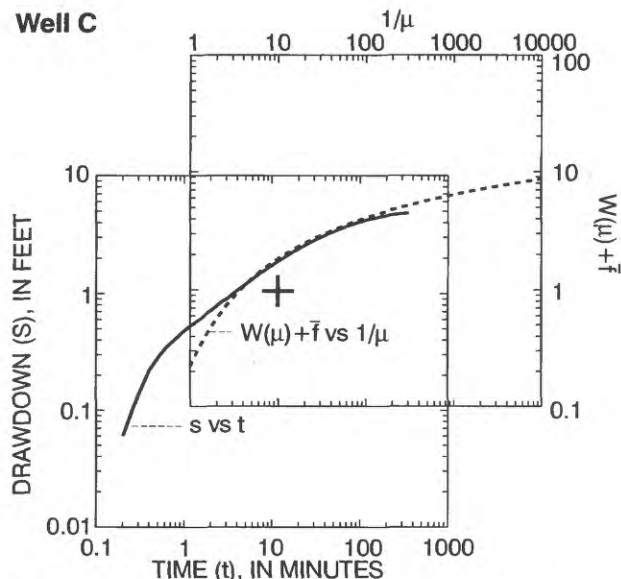
The dominant direction of linear terrain features in the area surrounding Duscree Creek is within an arc defined by the southeast (or northwest) quadrant (fig.

Well A



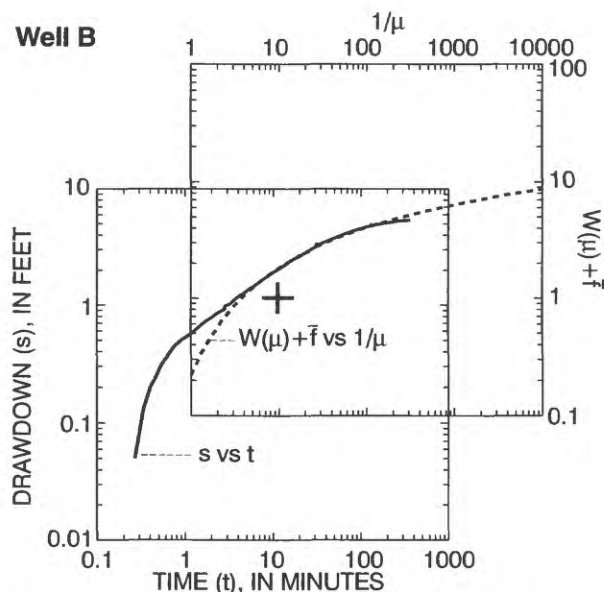
Match point coordinates for well A:  $W(\mu) + \bar{f} = 1$ ;  
 $s = 0.7$  feet  
 $\mu = 0.1$ ;  
 $t = 11$  minutes

Well C



Match point coordinates for well C:  $W(\mu) + \bar{f} = 1$ ;  
 $s = 1.1$  feet  
 $\mu = 0.1$ ;  
 $t = 12$  minutes

Well B



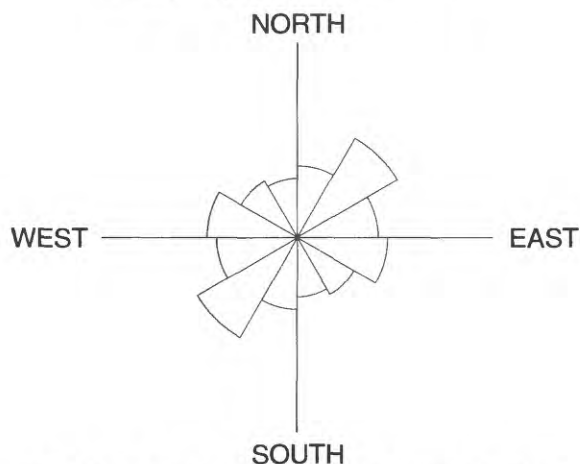
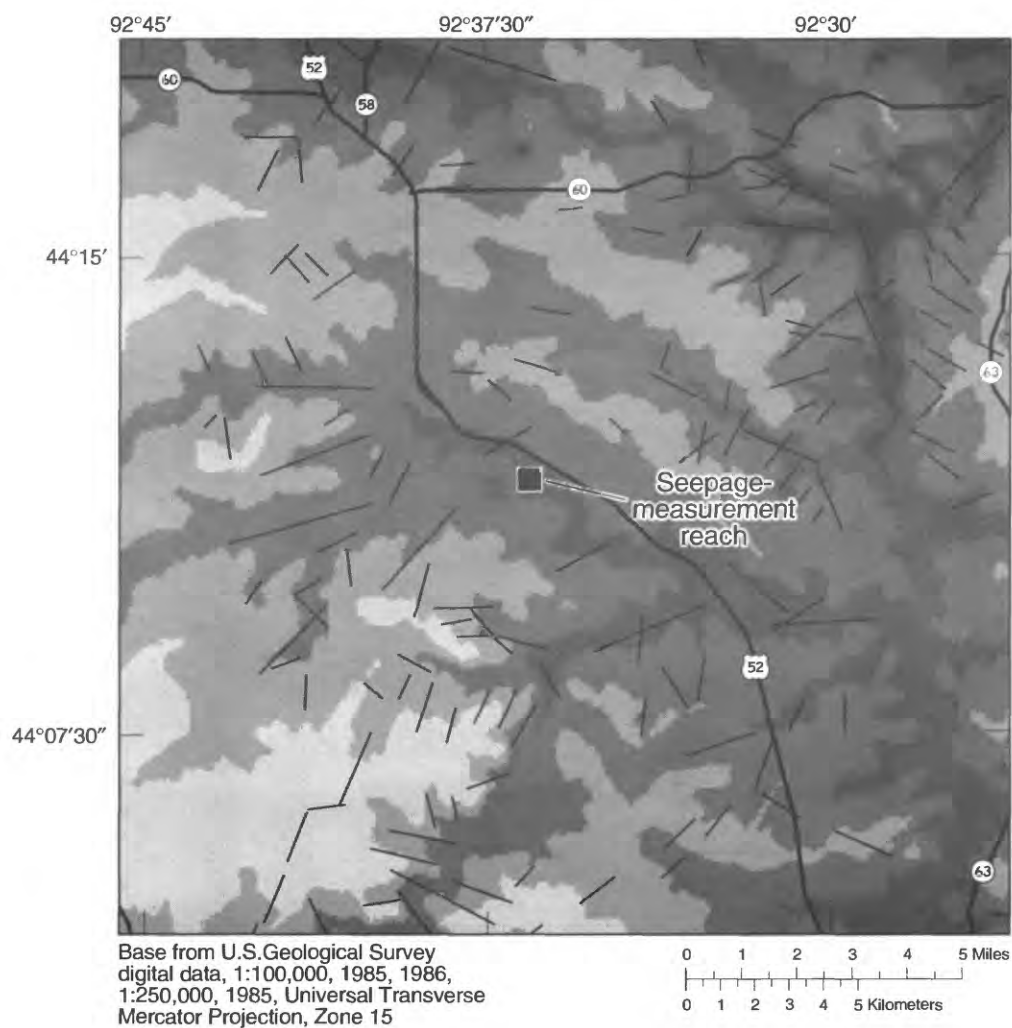
Match point coordinates for well B:  $W(\mu) + \bar{f} = 1$ ;  
 $s = 1.2$  feet.  
 $\mu = 0.1$ ;  
 $t = 12$  minutes

#### EXPLANATION

Match point values of  $W(\mu) + \bar{f}$ , ( $\mu$ ), drawdown ( $s$ ), and time ( $t$ ), were determined from the  $+$  shown on the overlying graphs

—  $s$  vs  $t$   
 - - -  $W(\mu) + \bar{f}$  vs  $1/\mu$

Figure 19.--Relation of the type curve  $[W(\mu) + \bar{f}]$  versus  $1/\mu$ , determined for a partially penetrating production well discharging at a constant rate of 240 gallons per minute from a nonleaky aquifer with a vertical to radial anisotropy of 100, to the time versus drawdown curve, for three observation wells used in an aquifer test of the St. Peter-Prairie du Chien-Jordan aquifer conducted November 12, 1989, near Rochester, Minnesota.



LINEAR TERRAIN FEATURE DIRECTIONS

Petals indicate directions of linear terrain features. Radial length of petals is proportional to number of observations within the petals.

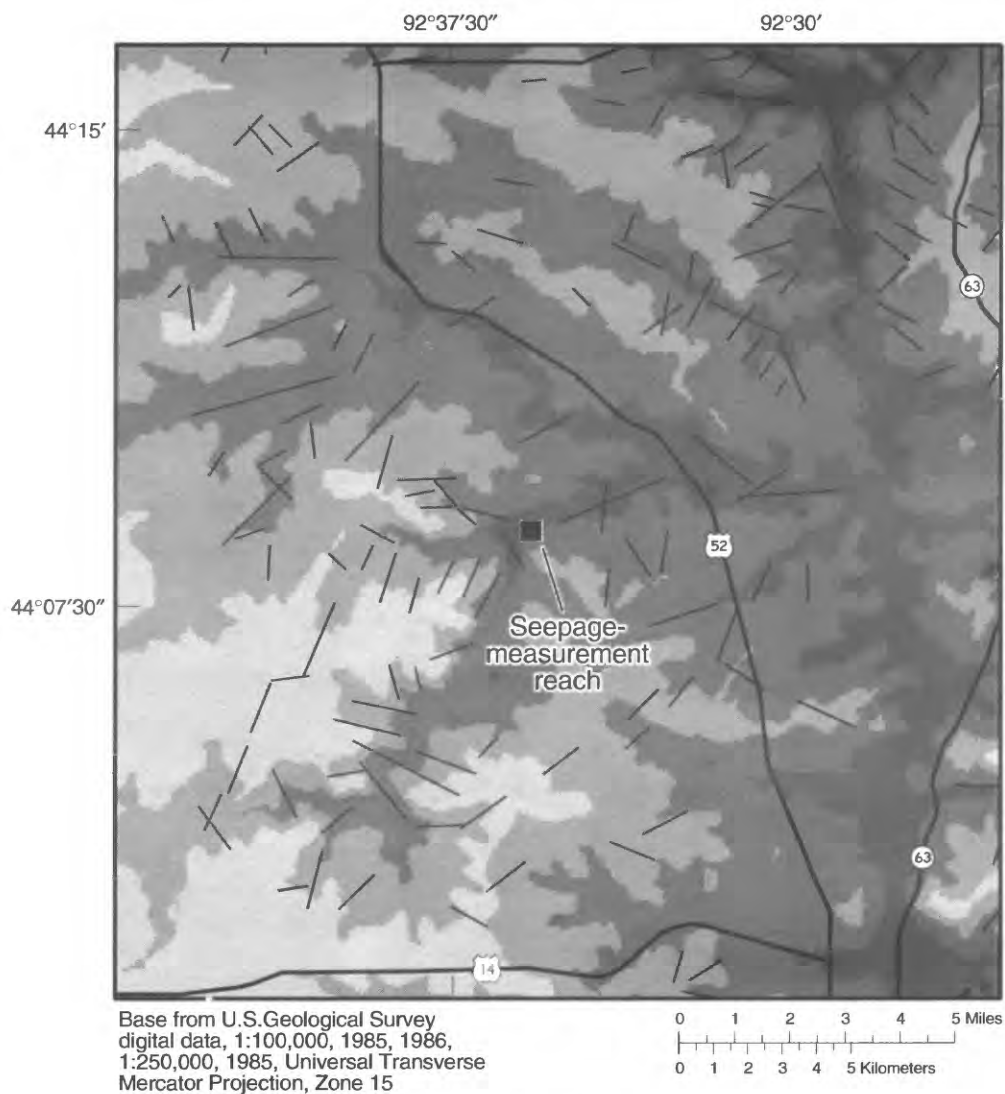
#### EXPLANATION

— Linear terrain feature

Elevation above sea level

FEET	METERS
1509	460
1411	430
1312	400
1214	370
1116	340
1017	310
919	280
820	250
722	220
610	186

Figure 20.—Rose diagram and linear terrain features in the area surrounding the seepage-measurement sites along the Middle Fork of the Zumbro River.



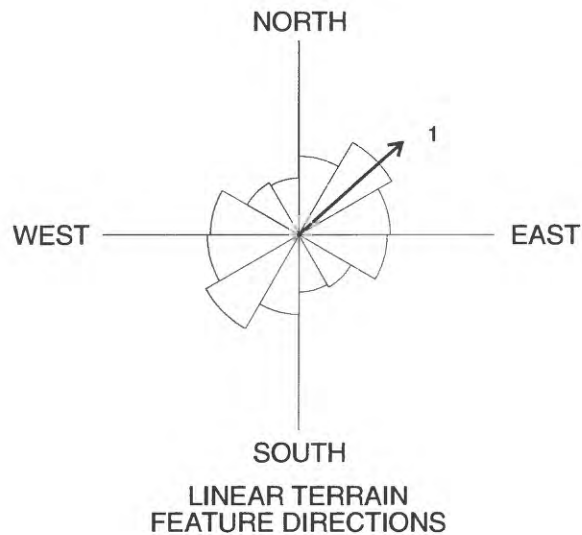
#### EXPLANATION

— Linear terrain feature

Elevation above sea level

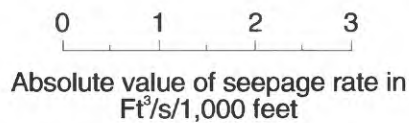
FEET	METERS
1509	460
1411	430
1312	400
1214	370
1116	340
1017	310
919	280
820	250
722	220
610	186

**Figure 21a.--Linear terrain features in the area surrounding the seepage-measurement sites along the South Branch of the Middle Fork of the Zumbro River.**

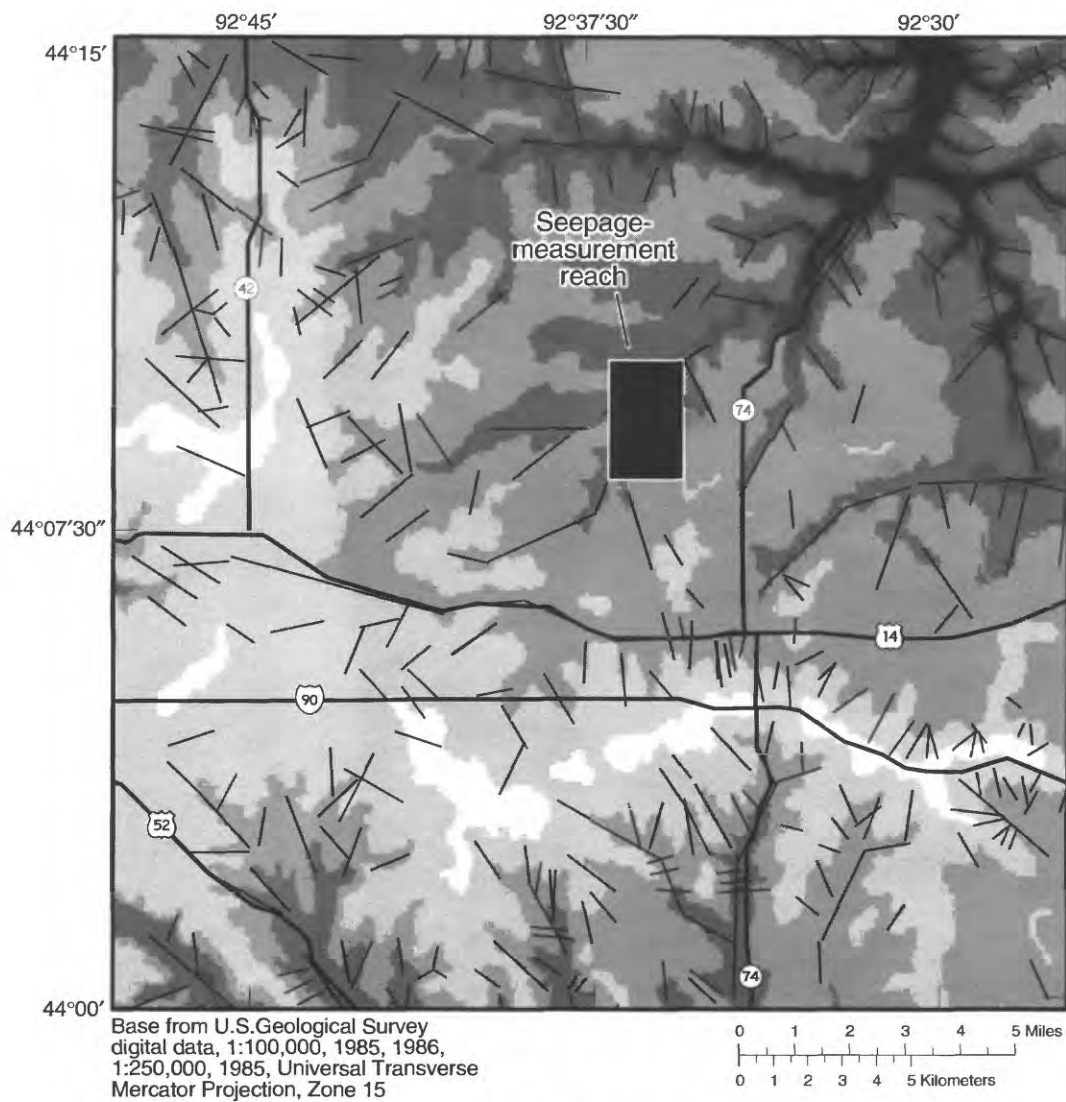


#### EXPLANATION

**Petals indicate directions of linear terrain features. Radial length of petals is proportional to number of observations within the petals. Arrow indicates the observation and flow direction of the stream reach used to measure seepage rate. Number by the arrow identifies the reach and corresponds to the reach number listed in table 1. The length of the arrow is directly proportional to the absolute value of the seepage rate. The following scale shows this relation.**



**Figure 21b.—Rose diagram of the linear terrain features in the area surrounding the seepage-measurement sites along the South Branch of the Middle Fork of the Zumbro River.**



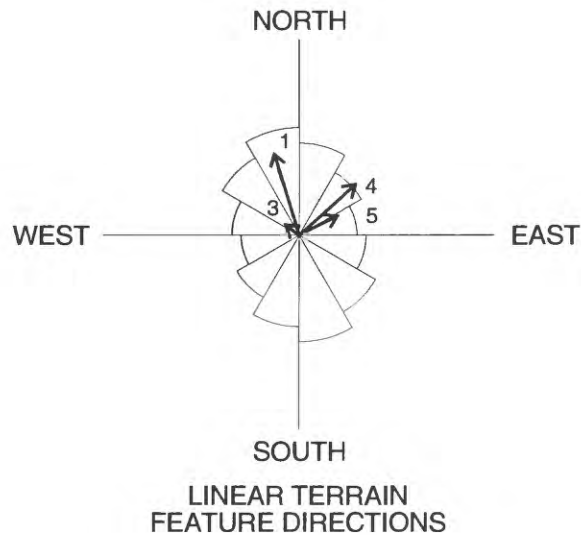
### EXPLANATION

— Linear terrain feature

Elevation above sea level

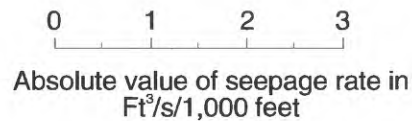
FEET	METERS
1509	460
1411	430
1312	400
1214	370
1116	340
1017	310
919	280
820	250
722	220
610	186

**Figure 22a.--Linear terrain features in the area surrounding the seepage-measurement sites along Crow Creek and the Middle Fork of the Whitewater River.**

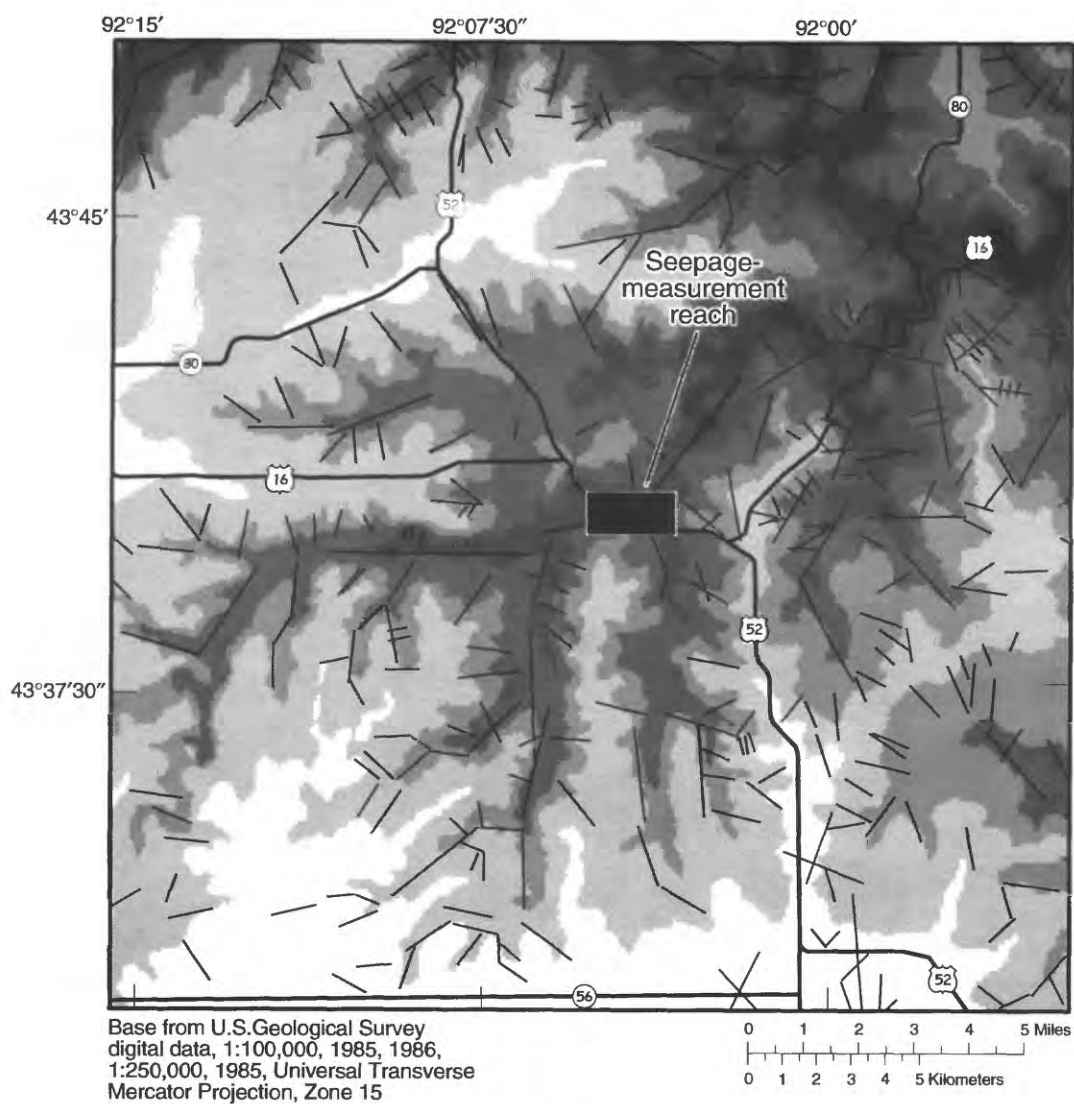


#### EXPLANATION

Petals indicate directions of linear terrain features. Radial length of petals is proportional to number of observations within the petals. Arrows indicate the observation and flow direction of the stream reaches used to measure seepage rate. Numbers by the arrows identify the reaches and correspond to the reach numbers listed in table 1. The length of the arrows is directly proportional to the absolute value of the seepage rate. The following scale shows this relation.



**Figure 22b.--Rose diagram of the linear terrain features in the area surrounding the seepage-measurement sites along Crow Creek and the Middle Fork of the Whitewater River.**

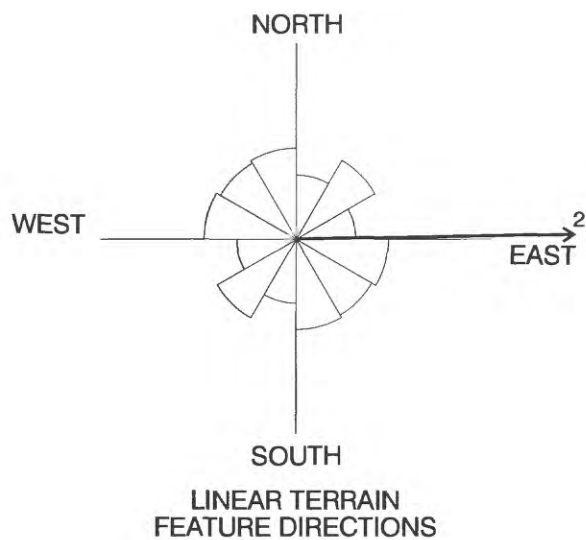


### EXPLANATION

— Linear terrain feature  
 — Elevation above sea level

FEET	METERS
1509	460
1411	430
1312	400
1214	370
1116	340
1017	310
919	280
820	250
722	220
610	186

**Figure 23a.—Linear terrain features in the area surrounding the seepage-measurement sites along the South Branch of the Root River.**

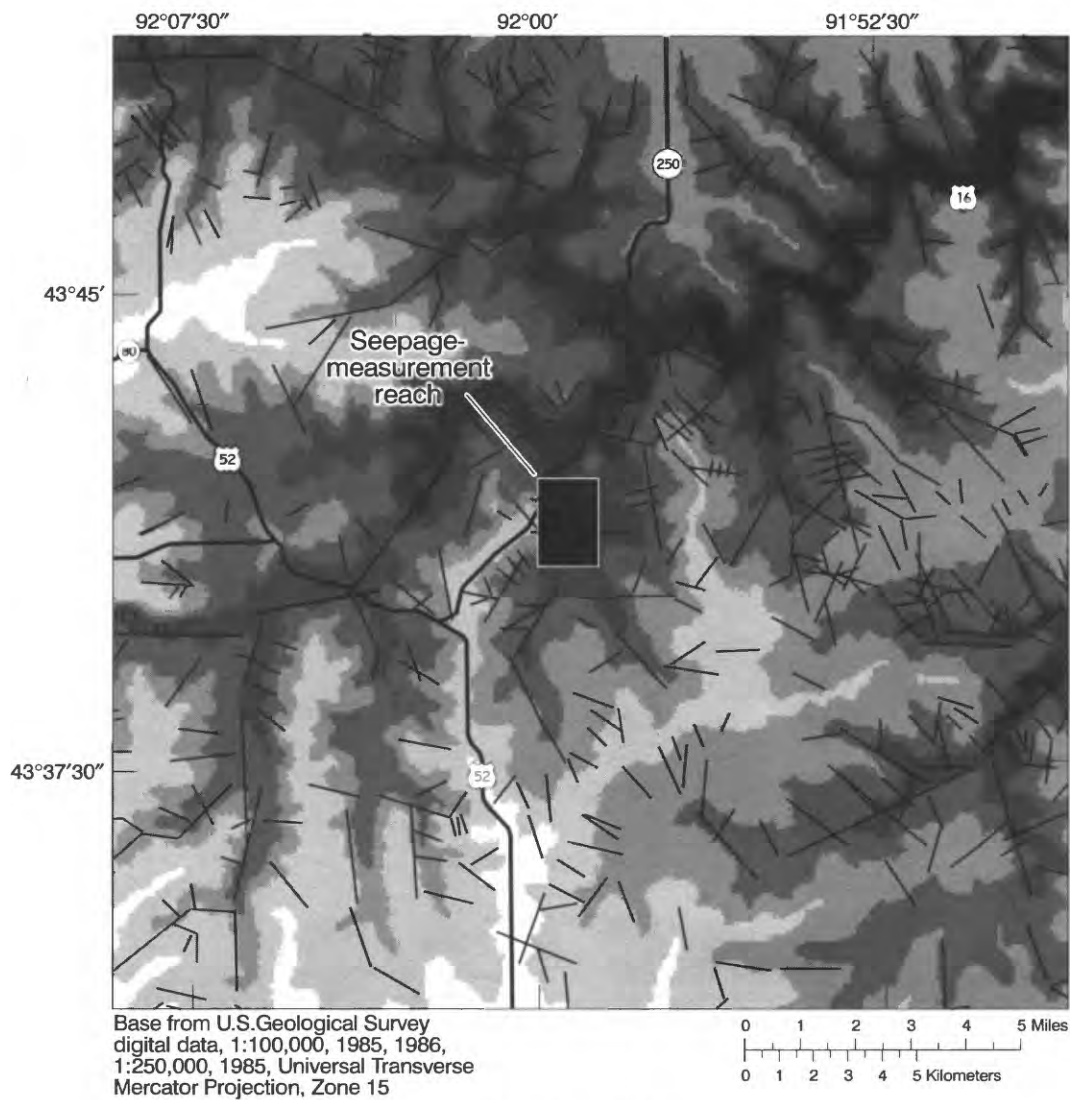


#### EXPLANATION

**Petals indicate directions of linear terrain features. Radial length of petals is proportional to number of observations within the petals. Arrow indicates the observation and flow direction of the stream reach used to measure seepage rate. Number by the arrow identifies the reach and corresponds to the reach number listed in table 1. The length of the arrow is directly proportional to the absolute value of the seepage rate. The following scale shows this relation.**



**Figure 23b.--Rose diagram of the linear terrain features in the area surrounding the seepage-measurement sites along the South Branch of the Root River.**



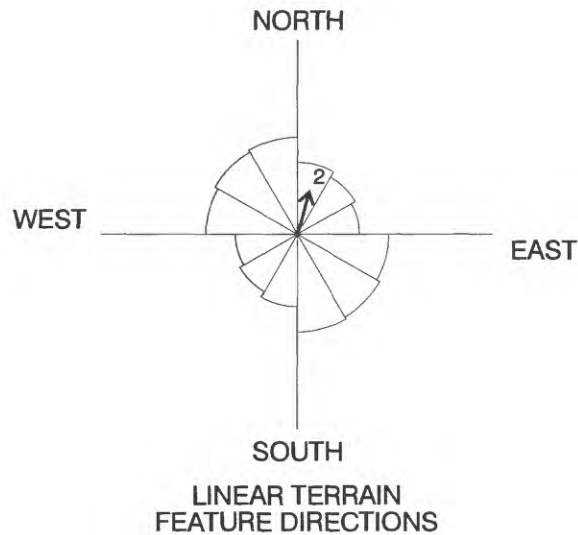
### EXPLANATION

— Linear terrain feature

Elevation above sea level

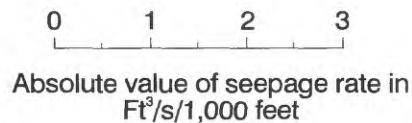
FEET	METERS
1509	460
1411	430
1312	400
1214	370
1116	340
1017	310
919	280
820	250
722	220
610	186

**Figure 24a.--Linear terrain features in the area surrounding the seepage-measurement sites along Duschee Creek.**

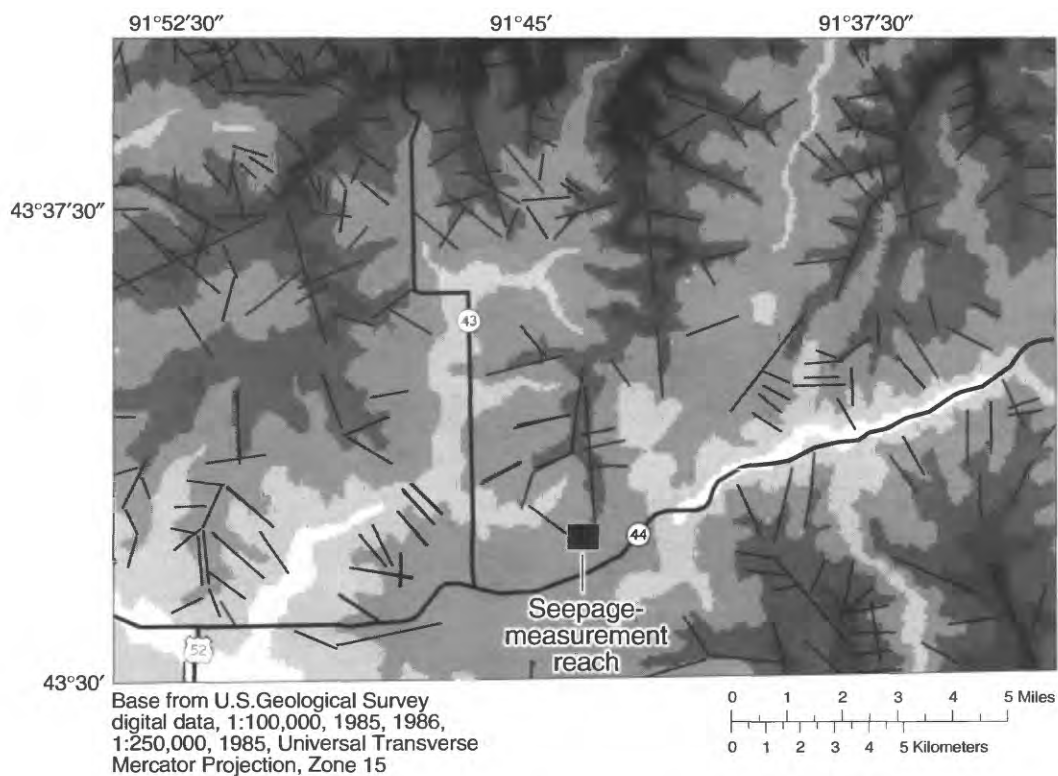


#### EXPLANATION

Petals indicate directions of linear terrain features. Radial length of petals is proportional to number of observations within the petals. Arrow indicates the observation and flow direction of the stream reach used to measure seepage rate. Number by the arrow identifies the reach and corresponds to the reach number listed in table 1. The length of the arrow is directly proportional to the absolute value of the seepage rate. The following scale shows this relation.



**Figure 24b.--Rose diagram of the linear terrain features in the area surrounding the seepage-measurement sites along Duschee Creek.**



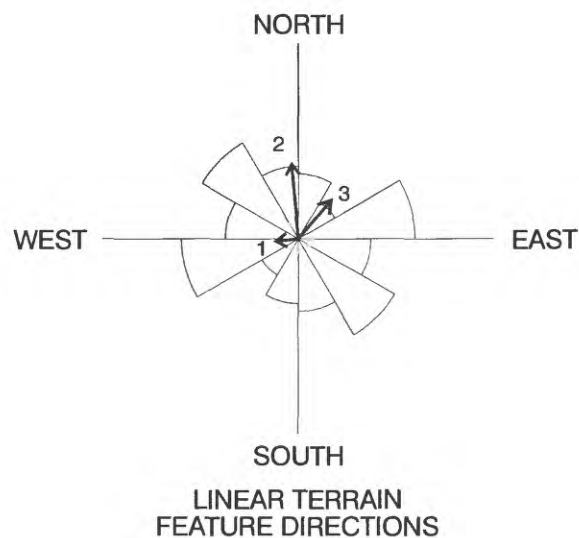
### EXPLANATION

———— Linear terrain feature

Elevation above sea level

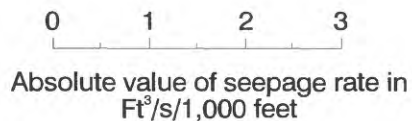
FEET	METERS
1509	460
1411	430
1312	400
1214	370
1116	340
1017	310
919	280
820	250
722	220
610	186

**Figure 25a.—Linear terrain features in the area surrounding the seepage-measurement sites along Riceford Creek.**



#### EXPLANATION

Petals indicate directions of linear terrain features. Radial length of petals is proportional to number of observations within the petals. Arrows indicate the observation and flow direction of the stream reaches used to measure seepage rate. Numbers by the arrows identify the reaches and correspond to the reach numbers listed in table 1. The length of the arrows is directly proportional to the absolute value of the seepage rate. The following scale shows this relation.



**Figure 25b.--Rose diagram of the linear terrain features in the area surrounding the seepage-measurement sites along Riceford Creek.**

Table 3.--Chi square statistic computed for linear terrain features interpreted from aerial photographs of areas shown in figure 5 that surround the seepage-measurement sites

[N, number of observations;  $X^2$ , chi square statistic; Significance is the probability that rejection of the null hypothesis, which is that the arcs of the rose diagrams in figures 20 through 25 have no directional trends, is in error. A significance value less than 0.0500 indicates rejection of the null hypothesis.]

Seepage-measurement site	N	$X^2$	Significance
Middle Fork of Zumbro River	156	8.239	0.1436
South Branch of the Middle Fork of the Zumbro River	154	7.431	.1905
Crow Creek and Middle Fork of Whitewater River	318	13.341	.0204
South Branch of Root River	326	9.264	.0990
Duschee Creek	423	13.355	.0203
Riceford Creek	252	26.602	.0001

24b). The largest rate of seepage was in reach 2, which is approximately aligned with the minor direction of local linear terrain features. The seepage rate for reach 1, which is aligned slightly clockwise from the direction of reach 2, was very small. The study hypotheses predict maximum seepage in reaches 1 and 2. These reaches are approximately aligned with the minor direction of the local linear terrain features. The seepage rate for reach 1 is inconsistent with the hypotheses, and the seepage rate for reach 2 is consistent.

The dominant direction of linear terrain features in the area surrounding Riceford Creek is defined by two arcs. One of these two arcs is within an east-west line and a line N60°E; the other arc is within a line N150°E and a line N120°E (fig. 25b). The largest and second largest seepage rates were in reaches 2 and 3, respectively, which are approximately aligned with the minor direction of local linear terrain features. The smallest seepage rate was in reach 1, which is approximately aligned with the dominant direction of local linear terrain features. The study hypotheses predict maximum seepage in reaches 2 and 3. The alignments of these reaches are at angles of 30 degrees or more to the dominant direction of local linear terrain features. The study hypotheses also predict minimum seepage in reach 1, which is approximately aligned with the dominant direction of local linear terrain features. The results for reaches 1, 2, and 3 are consistent with the hypotheses of the study.

## Summary

Ground-water flow in the karst-terrane aquifers of southeastern Minnesota is not well defined. Variable

fracture patterns in the bedrock strata affect permeability. Limestone and dolomite formations that are part of these aquifers typically exhibit secondary permeability because of these fractures, which allow open channel flow of ground water that is difficult to define without sufficiently detailed information about the orientations of the fractures.

Fracture patterns and seepage to streams were studied in the Prairie du Chien Group, which is the karst portion of the St. Peter-Prairie du Chien-Jordan aquifer, the principal aquifer in southeastern Minnesota. One hypothesis of the study is that the major axes of linear terrain features and of fractures in the Prairie du Chien Group are correlated. The other hypothesis of the study is that the principal axes of fractures in the Prairie du Chien Group and of seepage from the Prairie du Chien Group are correlated. The hypotheses were tested by comparing fracture orientations in the Prairie du Chien Group, local linear terrain features, and seepage to streams incised into the Prairie du Chien Group.

Exposures of the Prairie du Chien Group in quarries, road cuts, and stream valleys are extensive in southeastern Minnesota. Fracture orientations of the Prairie du Chien Group measured at 10 exposure sites indicate that the directional trends at eight of these sites are statistically significant. Linear terrain features identified in areas surrounding these sites exhibit statistically significant directional trends at four sites. Statistically significant directional trends of linear terrain features and fractures are common to three sites.

The fracture orientation measurements correlate with local linear terrain features at 2 of the 10 exposure sites. Results from the other eight sites are either unresponsive

or inconclusive about the postulated correlation of fractures and linear terrain features. Among these eight sites, directional trends of the linear terrain features are absent at five sites where directional trends of fractures are present, and directional trends of linear terrain features are present at one site where directional trends of fractures are absent. Directional trends of the two sources of data are both absent at one site, and directional trends of the two sources of data are both present, although different, at one site. These data generally do not validate the reliability of indirect estimates of bedrock fracture patterns based on interpretation of linear terrain features except possibly where these features exhibit significant directionality.

An aquifer test designed to determine local anisotropy in the karst portion of the St. Peter-Prairie du Chien-Jordan aquifer indicates that the major axis of horizontal transmissivity is along a line that is N95°E. This axis is assumed to correspond to the major axis of the fractures because the most preferred direction of ground-water flow is likely to be in a direction parallel to the fractures.

Seepage along stream reaches at six sites and local linear terrain features are weakly supportive or inconclusive about the postulated correlation of fractures and seepage. Data from Crow Creek and the Middle Fork of the Whitewater River and from Duschee Creek are inconclusive. Data from Riceford Creek indicate that the seepage was higher to reaches that cut across the directional trends of linear terrain features at angles of 30 degrees or more, thus the data from this site support the hypotheses of the study. The hypotheses could not be tested with the data collected at the Middle Fork of the Zumbro River, the South Branch of the Root River, and the South Branch of the Middle Fork of the Zumbro River because the linear terrain features lack directional trends.

Prediction of seepage may be possible in areas where local linear terrain features exhibit directional trends. Such predictions, however, are likely to be useful only in reconnaissance-level studies where the uncertainty of the predictions are understood and accepted. The difficulties encountered in this study to describe fracture patterns and seepage from the Prairie du Chien Group indicate the complexity of the hydrogeology of karst-terrane aquifers in southeastern Minnesota.

## References

- Broussard, W.L., Farrell, D.F., Anderson, H.W., Jr., and Felsheim, P.E., 1975, Water resources of the Root River watershed, southeastern Minnesota: U.S. Geological Survey Hydrologic Investigations Atlas HA-548, 3 pl., scale 1:250,000.
- Dalgleish, J., and Alexander, E.C., Jr., 1984, Hydrogeologic investigation of the proposed expansion site of the Winona County (Murphy) landfill: Department of Geology and Geophysics, University of Minnesota, Minneapolis, Minnesota, 34 p.
- Delin, G.N., and Woodward, D.G., 1984, Hydrogeologic setting and the potentiometric surfaces of regional aquifers in the Hollandale Embayment, southeastern Minnesota, U.S. Geological Survey Water-Supply Paper 2219, 56 p.
- Hantush, M.S., 1964, Hydraulics of wells, in Chow, Ven Te, ed., *Advances in Hydrosience*, Volume 1: New York, Academic Press, p. 281-442.
- Hobbs, H.C., 1984, Surficial Geology, in Balaban, N.H., and Olsen, B.M., eds., *Geologic Atlas Winona County, Minnesota: Minnesota Geological Survey, County Atlas Series, Atlas C-2, plate 3*, scale 1:100,000.
- , 1988, Surficial Geology, in Balaban, N.H., ed., *Geologic Atlas Olmsted County, Minnesota. Minnesota Geological Survey, County Atlas Series, Atlas C-3, plate 3*, scale 1:100,000.
- Kanivetsky, R., 1984, Bedrock Hydrogeology, in Balaban, N.H., ed., *Geologic Atlas Winona County, Minnesota: Minnesota Geological Survey, County Atlas Series, Atlas C-2, plate 4*, scale 1:100,000.
- King, P.T., Michel, J., and Moore, W.S., 1982, Ground water geochemistry of  $^{228}\text{Ra}$ ,  $^{226}\text{Ra}$ , and  $^{222}\text{Rn}$ , *Geochimica et Cosmochimica Acta*, v. 46, p. 1173-1182.
- Lattman, L.H., 1958, Technique of mapping geologic fracture traces and lineaments on aerial photographs, *Photogrammetric Engineering*, v. 24, p. 568-576.
- Lattman, L.H., and Parizek, R.R., 1964, Relationship between fracture traces and the occurrence of ground water in carbonate rocks, *Journal of Hydrology*, vol. 2, p. 73-91.

Lee, R.W., and Hollyday, E.F., 1987, Radon measurement in streams to determine location and magnitude of ground-water seepage, *in* Graves, B., ed., *Proceedings of National Water Well Association Conference*: Lewis Publishers, Inc., Somerset, New Jersey, p. 241-249.

Maslia, M.L., and Randolph, R.B., 1987, Methods and computer program documentation for determining anisotropic transmissivity tensor components of two-dimensional ground-water flow: U.S. Geological Survey Water-Supply Paper 2308, 46 p.

Mohring, E.H., and Alexander, E.C., 1986, Quantitative tracing of karst ground-water flow, southeastern Minnesota, north-central United States, Publication 1100 of the School of Earth Sciences: Department of Geology and Geophysics, University of Minnesota, Minneapolis, Minnesota, 20 p.

Mossler, J.H., and Book, P.R., 1984, Bedrock Geology, *in* Balaban, N.H., and Olsen, B.M., eds., *Geologic Atlas Winona County, Minnesota*: Minnesota Geological Survey, County Atlas Series, Atlas C-2, plate 2, scale 1:100,000.

Olsen, B.M., 1988, Bedrock Geology, *in* Balaban, N.H., ed., *Geologic Atlas Olmsted County, Minnesota*: Minnesota Geological Survey, County Atlas Series, Atlas C-3, plates 2 and 4, scale 1:100,000.

Papadopoulos, I.S., 1965, Nonsteady flow to a well in an infinite anisotropic aquifer, *Proceedings of the Dubrovnik Symposium on the Hydrology of Fractured Rocks*: International Association of Scientific Hydrology, p. 21-31.

Porcher, E., 1989, Ground-water contamination susceptibility in Minnesota: Minnesota Pollution Control Agency, revised edition, 29 p.

Reed, J.E., 1980, Type curves for selected problems of flow to wells in confined aquifers: U.S. Geological Survey Techniques of Water-Resources Investigations, book 3, chap. B3, 106 p.